

**HYPERBOLIC AUTO-NAVIGATION**

**BY**

**WESLEY MATTHEW THORSSON**

Thesis  
T46

100 Y  
U. S. Naval Postgraduate School  
Annapolis, Md.

DUDLEY KNOX LIBRARY  
NAVAL POSTGRADUATE SCHOOL  
MONTEREY, CALIFORNIA 93943-5002







HYPERBOLIC AUTO-NAVIGATION

-

W. 'M. Thorsson





HYPERBOLIC AUTO-NAVIGATION

By

Wesley Matthew Thorsson,  
Lieutenant (jg), United States Coast Guard

Submitted in partial fulfillment  
of the requirements  
for the degree of  
MASTER OF SCIENCE

United States Naval Postgraduate School  
Annapolis, Maryland  
1950

Thesis  
T 46

This work is accepted as fulfilling  
the thesis requirements for the degree of

MASTER OF SCIENCE

from the  
United States Naval Postgraduate School.



## PREFACE

The purpose of this paper will be to give the reader a general description of possible methods of automatic navigation by hyperbolic systems, and their possible advantages and failings. A report on the circuitry and operation of one type of computer is given to demonstrate possible methods of attack for the problem, and the steps taken in this specific example to achieve the required accuracy of such a computer. A preliminary model of a vector analog course computer was designed and constructed at Sperry Gyroscope Company at Great Neck, New York, during 1949, and 1950. During the period of 3 January, 1950 till 17 March of the same year, it was my pleasure to assist in the construction, and testing of this computer. With little exception, all information gathered for this paper was gathered during this period from the engineering reports and laboratory note books of Sperry Gyroscope Company engineers, or from personal observations. I am indebted to Robert Frank, the head of this project, Wilbert Frantz, other engineers of the corporation, and Technician Rudolph Jamross for their assistance to me in pursuing this subject.



# TABLE OF CONTENTS

<u>Chapter</u>	<u>Subject</u>	<u>Page</u>
I	Introduction	1
II	Digital Computer	3
III	Lorhumb Computer	6
IV	Streeter Automatic Navigator	13
V	Hyperbolic Position Recording and Plotting Systems	15
VI	Vectorial Analog Hyperbolic Course Computer	16
VII	Choice of a System for Construction	21
VIII	Circuit Description of Vector Computer	22
	1. Oscillator	22
	2. Phase Shifter Chassis	22
	3. Time Difference and Station Base Chassis	24
	4. Isolation Amplifiers	28
	5. Detector Sub Chassis	28
	6. Servo Amplifier	31
	7. Phase Detector	34
IX	Predicted Effects of System Errors	36
	1. Phase Shift in $R_{Cref}$	36
	2. Phase Shift in $R_C$	36
	3. Effect of an Unbalance of Phase Detector of Course Servo	36
	4. Effect of Non-intersection of Hyperbolas	37
	5. Effect of Error in Station Vectors	38
	6. Effect of Nonlinearities of Detectors	38





TABLE OF CONTENTS  
(Cont.)

<u>Chapter</u>	<u>Title</u>	<u>Page</u>
X	Laboratory Tests of Computer	40
	1. Oscillator	40
	2. Phase Shifter Chassis	40
	3. Time Difference and Station Base Chassis	41
	4. Isolation Amplifiers	43
	5. Detector Sub-Chassis	43
	6. Servo Amplifier	45
	7. Phase Detector	45
	8. System Performance	45
XI	Conclusion	48
	Appendix A	49
	Appendix B	53
	Bibliography	57



## LIST OF ILLUSTRATIONS

<u>Figure</u>	<u>Title</u>
I(A)	Spherical Triangles for Hyperbolic Problem.
I(B)	Source Impedance of $T_W$ .
I(C)	Time Difference Error Sensitivity of Correcting $R_X$ .
II	Digital Block Diagram.
III	Lorhumb Computer Mechanical Block Diagram.
IV	Lorhumb Electronic Computer Block Diagram.
V	Lorhumb Lines.
VI	Streeter Computer Block Diagram.
VII	Vector Diagram of Hyperbolic Vector Computer.
VIII	Hyperbolic Coordinate Chart of Newfoundland.
IX	Vector Computer Block Diagram.
X	Oscillator.
XI	Phase Shifter Chassis.
XII	Time Difference and Station Base Line Chassis.
XIII	Isolation Amplifier.
XIV	Detector Sub Chassis.
XV	Servo System.
XVI	Sum and Difference of Time Differences: Example 1.
XVII	Sum and Difference of Time Differences: Example 2.
XVIII	Phase Detector.
XIX	Old Detector Chassis.
XX(A)	Phase Shift in $R_{c\text{ref}}$ .
XX(B)	Phase Shift in $R_c$ .



LIST OF ILLUSTRATIONS  
(cont.)

<u>Figure</u>	<u>Title</u>
XX(C)	Unbalance of Phase Detector.
XXI	Path Due to Parallel Hyperbolas.
XXII	Path Due to 30 Degree Error in Station Bases.
XXIII	Track of Computer in Plane.
XXIV	Projections of Great Circles on Vector Plane.
XXV	Loran Autonavigator, Front View.
XXVI	Loran Autonavigator, Rear View, Shields Removed.
XXVII	Loran Autonavigator, Rear View.



LIST OF SYMBOLS AND ABBREVIATIONS  
AS THEY APPEAR IN THE TEXT

$\beta$	Angle from meridian to the arc from the central station to the craft position.
$S_x, S_y, \text{ and } S_w.$	Arc lengths to the position of the craft from stations x, y, and w respectively.
$\sigma_x, \sigma_y, \text{ and } \sigma_w.$	Angles subtended at the center of the earth by $S_x, S_y, \text{ and } S_w$ respectively.
$L_r, L_y, L_x, L_w, L_d.$	Latitudes of position R, stations y, x, w and destination d respectively.
$\lambda_r, \lambda_y, \lambda_x, \lambda_d.$	Longitudes of r, y, x, and d respectively.
a	Equatorial radius of the earth.
f	Measure of oblateness of the earth.
$\Delta S_x$	Oblateness correction to $a\sigma_x$ to obtain arc length on the earth.
$TD_{xy}$	Difference of distances $S_x$ and $S_y$ or of the times proportional to these distances.
$TD_{xw}$	Difference of distances $S_x$ and $S_w$ or of the times proportional to these distances.
$Y_d$	Difference in time differences $TD_{xy}$ for position and destination.





LIST OF SYMBOLS AND ABBREVIATIONS  
AS THEY APPEAR IN THE TEXT  
(cont.)

Wd	Difference in time differences TD <sub>xw</sub> for position and destination.
K	Ratio of Yd and Wd.
$\theta_a$	Angle between arcs XY and Sx.
K <sub>y</sub>	Equal to S <sub>y</sub> - S <sub>x</sub> .
K <sub>w</sub>	Equal to S <sub>w</sub> - S <sub>x</sub> .
W	Angle subtended by the arc between stations X and W at the center of the earth.
Y	Angle subtended by the arc between stations X and Y.
n	Constant introduced into Streeter computer so all multipliers will be less than unity.
$\theta$	Angle between meridian and arc S <sub>y</sub> .
d	Miles deviation from desired track.
q	Proportionality constant relating angular and linear measurements on the surface of the earth.
$\tau$	Angle between rhumb track and meridian.
XW and XY	Vectors representing distances and angles from station X to W or Y respectively.
R <sub>xd</sub> , R <sub>xp</sub>	Vectors representing distance and angle to the destination and position respectively, or the voltage representing that vector.



LIST OF SYMBOLS AND ABBREVIATIONS  
AS THEY APPEAR IN THE TEXT  
(cont.)

$R_{yd}, R_{yp}$	Vectors from station Y to the destination and position, or the voltage representing that vector.
$R_{wd}, R_{wp}$	Vectors from stations W to the destination and position, or the voltage representing the vector.
$R_c$	Vector from the position to destination, or the voltage representing it.
$R_{c\text{ref}}$	The vector set up to correspond to the initial $R_c$ . The voltage $R_{c\text{ref}}$ representing the vector is in quadrature with it.
$T_{xp}, T_{xd}$	Times corresponding to arc length $S_{xp}$ and $S_{xd}$ .
$R_{dl}, C_{dl}$	Compensation resistance and capacitance to keep load on $R_{xd}$ output constant.
$E_{\text{ref}}$	Reference voltage supplied by oscillator.
$T_x, T_y, T_w$	Times proportional to $S_x, S_y$ and $S_w$ .
$B_w, B_x, B_y$	Voltage representing the station base vector $XW$ , the quadrature and in phase components of $XY$ respectively.



## I INTRODUCTION

With the increasing speed of aircraft, and the need for self-navigation of missiles for military use, a long range automatic navigation system has become increasingly more desirable. The use of a hyperbolic system of navigation reduces the possible errors inherent in systems of the direction finding type. Since the direction of the incoming phase front is not important, distortions in its direction caused by varying paths to the craft, or by distortions of the field by the craft itself, cause no error. These hyperbolic systems locate position by measurement of the time differences between the arrival of two signals. It is well known that the loci of points of constant difference of distances from two fixed points are hyperbolas. Therefore, by measuring the time differences between the arrival of signals from two pairs of stations, the position is fixed at the intersection of the two hyperbolas representing those time differences. These differences may be obtained from systems such as Loran, Decca, GEE, Raydist, or Lorac. Any of these systems may be engineered so as to automatically present the time differences in the form of shaft rotations proportional to time differences.

For an automatic navigator having these shaft rotations for inputs, along with a knowledge of the location of the stations, the requirements of the system might be:





- (1) Control of the course of the craft to cause it to follow a predetermined route to a destination and indication of the amount of deviation from that route.
- (2) Indication of distance or time remaining until the craft reaches the destination.
- (3) Indication of the position of the craft at any time, and possibly a plot of these positions.
- (4) Initiation of some procedure upon arriving at a certain distance from the destination.

The systems which might be used to accomplish several or all of these requirements may be classified as either digital or analog computer types. The most accurate information is obtainable from a digital system, but is obtained at the expense of simplicity and increasing bulk. Descriptions of computers of each type and a detailed description of the circuits for one computer will be given.





## II DIGITAL COMPUTER

A digital computer is proposed by Winslow Palmer<sup>3</sup> of the Sperry Gyroscope Company in the report, "Project Report Study of Loran Digital Computer". Such a computer should be accurate to one part in 100,000 in each element in order not to degrade the information available from Loran. Using a binary system, this calls for the use of 17 digits with 11 storage elements capable of storing these 17 digits for further use. Figure I(A) shows the spherical triangle to be solved by assuming a position, calculating the time differences from this position to the three stations, comparing these to the observed time differences, and correcting the position accordingly. The remaining information, such as position in latitude and longitude, course to destination, deviation from this desired course, and time and distance remaining to the destination are then calculated. The steps taken in computation with the formulas used<sup>3</sup>, assuming  $\beta$  and  $S_x$  known, and calling the angles subtended by the arcs  $S_x$ ,  $S_y$ , and  $S_w$ ,  $\phi_x$ ,  $\phi_y$  and  $\phi_w$  respectively are:

- (1) Find  $L_r$ , the latitude of point R.

$$L_r = \sin^{-1} \left[ \cos \phi_x \sin L_x + \sin \phi_x \cos L_x \cos \beta \right]$$

- (2) Find  $\lambda_r$ , the longitude of point R.

$$\lambda_r = \lambda_x - \sin^{-1} \left[ \frac{\sin \phi_x \sin \beta}{\cos L_r} \right]$$



(3) Find  $\sigma_x$

$$\sigma_x = \cos^{-1} \left[ \sin L_x \sin L_r + \cos L_x \cos L_r \cos (\lambda_x - \lambda_r) \right]$$

(4) Find  $\Delta S_x$ , the oblateness correction for  $\sigma_x$ .

$$\Delta S_x = \frac{af}{2} \left[ \begin{array}{l} \frac{3 \sin \sigma - \sigma}{\cos^2 \frac{\sigma}{2}} \sin^2 \left( \frac{L_1 + L_2}{2} \right) \cos^2 \left( \frac{L_1 - L_2}{2} \right) \\ - \frac{3 \sin \sigma + \sigma}{\sin^2 \frac{\sigma}{2}} \cos^2 \left( \frac{L_1 + L_2}{2} \right) \sin^2 \left( \frac{L_1 - L_2}{2} \right) \end{array} \right]$$

where  $L_x$  and  $L_r$  are the latitudes of points X and R, and  $\sigma_x$  the angle subtended by the distance  $S_x$ .

(5) Find  $S_x$ .

$$S_x = a \sigma_x + \Delta S_x$$

where  $a$  is the equatorial radius of the earth and  $f$  is a measure of the oblateness of the earth in the area.

(6) Repeat steps (3), (4), and (5) for  $S_y$  and  $S_w$ .

(7) Find the time difference  $TD_{xy}$ .

$$TD_{xy} = S_x - S_y$$

(8) Find the time difference  $TD_{xw}$ .

$$TD_{xw} = S_x - S_w$$

A block diagram of the system is shown in Figure II, and will be described below. A cycling unit instructs as to the sequences to be followed, and an arithmetic unit adds, subtracts, multiplies, or divides as instructed.



An assumed  $\sigma_x$  and  $\beta$  are transmitted when needed; and for them, the corresponding time differences are found and compared with the observed differences. Then  $\sigma_x$  and  $\beta$  are corrected to give a zero error in the time differences. The total time taken to perform this operation is about 0.3 seconds if only ten terms are required to represent the inverse sine to the desired accuracy, but when, under some conditions, the inverse sine requires 100 terms before converging sufficiently, the time required for a solution may be over 2.0 seconds, allowing five microseconds for each pulse operation. The computer by present techniques would fill four or five telephone racks, but could be made much smaller with careful engineering.





### III LORHUMB COMPUTERS

In any hyperbolic system, a point is located by its two hyperbolic coordinates. These coordinates are designated in this paper as time differences  $TD_{xy}$  and  $TD_{xw}$ . A lorhumb line<sup>4</sup> is a line passing through such a coordinate system so that the ratio of the rate of decrease of  $TD_{xy}$  to the rate of decrease of  $TD_{xw}$  will be constant. A simple way of obtaining a lorhumb line that will pass through a point representing present position and through a point representing the desired destination is given by Frantz<sup>2</sup>. To plot the lorhumb line, a rephrasing of the definition of the line is used as given below. A lorhumb line is a line for which the ratio of the difference between  $TD_{xy}$  for the destination and  $TD_{xy}$  for the position to the difference of  $TD_{xw}$  for the destination and  $TD_{xw}$  for the position remains constant. Then, to run a lorhumb line to the destination from present position, obtain the differences in the  $TD_{xy}$  coordinates of present position and of the destination, repeat for the  $TD_{xw}$  coordinates, and obtain the ratio of the two differences. For points along the path, select a  $TD_{xw}$ , subtract it from the destination  $TD_{xw}$ , multiply the difference by the ratio obtained above, and subtract this new difference from the  $TD_{xy}$  for the destination to obtain the  $TD_{xy}$  for the point desired.

A lorhumb computer operates to cause the craft to follow a lorhumb line to the destination. Several examples of lorhumb lines may be found in MIT Radiation Laboratory





Series #4, "Loran" on pages 112 to 115<sup>4</sup>. These lines show the most obvious failing of the system, that is, departure from a reasonable great circle course. If this can be overlooked, however, this promises to be one of the simplest computers to construct. Several types have been proposed, two of which will be described here.

The mechanical Lorhumb computer shown as a block diagram in Figure III has for inputs the time differences of the destination, and the continuous time differences of present position. These time differences are subtracted in a mechanical differential, the output for the XY differences being designated  $y_d$ , and that of the XW differences,  $w_d$ . In a mechanical multiplier,  $y_d$  is multiplied by a constant  $k$ , and the output,  $ky_d$  is subtracted from  $w_d$  in a differential. The difference, equal to the error in  $ky_d$ , is indicated on a dial, and also used as an input to a servo amplifier. At the start of the problem, the output of the servo is switched to a motor, which is controlled to change the multiplying constant  $k$  so as to make the error output zero. This, then establishes the ratio of time differences,  $k$ , which is to be held constant. The output of the servo amplifier is now switched to the autopilot, which changes the course thereafter so as to maintain the error output zero. This system has several failings. First, if  $k$  is either very large or very small, the accuracy of multiplication would probably not be great enough. Also, as  $y_d$  and  $w_d$



become small, the sensitivity of detecting errors in the ratio would decrease. This might be overcome by shifting the time difference inputs, when both  $y_d$  and  $w_d$  become less than a certain amount, to a set of gears that would again make the values  $w_d$  and  $y_d$  as large as at the start of the problem.

The electrical lorhumb computer, illustrated as a block diagram in Figure IV, also obtains differences in time differences  $y_d$  and  $w_d$ , by either mechanical or electrical differentials (shown as mechanical in Figure IV). The differences  $y_d$  and  $w_d$  are applied through isolation amplifiers to windings on a synchro spaced ninety degrees mechanically. The output of one winding of the rotor is applied to a servo amplifier, which at the start of the problem controls a motor that turns the rotor until the rotor output is zero. This angle of the rotor is dependent upon the relative magnitudes impressed on the two windings, and therefore fixes the ratio of the differences  $y_d$  and  $w_d$ . The servo amplifier is then switched to the autopilot, which guides the craft so as to maintain the rotor output equal to zero. The second rotor winding output is used in an automatic gain circuit, which keeps the sensitivity of the servo amplifier about constant as  $w_d$  and  $y_d$  become smaller. Errors in the space position of the rotor for a null in this system would cause deviation from a lorhumb line, but would still bring about convergence to the destination on a new lorhumb line, providing such a line exists. A possible limitation



in the accuracy of arriving at the destination is the resistance resolution of the potentiometers. Helipot's are commercially available having 40 turns of the rotor, passing over 100,000 turns of wire. The resolution then could be 1 part in 100,000. As the destination is approached, again  $y_d$  and  $w_d$  become small, tending to decrease the percent accuracy of the servo system's ability to maintain a constant ratio of  $w_d$  to  $y_d$ . In this case, either the input time differences could be shifted to geared up outputs or the gain of the isolation amplifiers could be increased as both  $w_d$  and  $y_d$  decrease below a given amount.

The lorhumb systems, then, are relatively simple, capable of a homing accuracy limited only by the resolution of the receiver and by the accuracy of the hyperbolic system. However, the course determined is not a great circle. Pierce<sup>4</sup> infers that lorhumb tracks between two points may always be found and that travel over such a track will result in not more than 10 percent excess path length over that for a great circle path between the two points. Data on several lorhumb tracks that were computed for this paper are included in Appendix A. To avoid plotting great circles for comparison, courses were taken either beginning and ending on the same meridian or on a base line extension for another loran pair since these lines are always great circles. The first three cases were worked for loran triplets with courses not near base lines. Path lengths less than 5 percent in excess over





the great circle path resulted. This seems an average value for courses determined in this manner. However, case 4, which had the same departure and arrival points as case 3, but utilizing time differences from two separate station pairs whose base lines were about parallel, had a track which failed to reach the destination. Using a second combination of two station pairs for this same track in case (5), again the lorhumb line failed to reach the destination. It appears that when the great circle crosses loran lines that are parallel, there is a possibility of no solution, since the lorhumb line time difference ratio may call for the intersection of parallel lines. In following the line in these cases, such a point was avoided by tracking on the wrong side of a base line extension which eventually lead to the alternate intersection of the hyperbolas involved.

In case (6) a course was laid on the same great circle as for cases 3, 4, and 5, having a destination just short of the parallel hyperbolas and using the same stations as used for case 5. In this case, the destination was reached with 12 percent excess travel.

For case 7, a triplet was chosen with a course crossing a position having parallel hyperbolas. Again, the lorhumb track led to the alternate intersection of hyperbolas from that desired. Cases 8 and 9 were chosen with the same departure point used in case 7 and with destinations on the same great circle, short of the point where the hyperbolas





were parallel. These led to proper destinations, with excess path lengths of 8.2, and 21 percent. These last three tracks are plotted in Figure V.

Lorhumb tracks, then, may not be used for tracks crossing base line extensions, or where the hyperbolas are parallel. The possibilities of no solution are greater when using two pairs of stations rather than a triplet, and for a triplet they increase with decreasing angle between the station base lines. Also, deviations from a great circle course will be greatest where the great circle to the destination crosses hyperbolas whose time differences first increase and then decrease in value or vice versa, rather than continuously increase or decrease. This is true since lorhumb lines are constrained to continuously decreasing difference of time differences of position and destination. Thus the lorhumb line may not cross the same time difference line twice, and therefore, may never cross the base line extension. Any lorhumb line going from a position on one side of a base line extension to a destination on the other side would be a very poor course to follow. Families of lorhumb lines for which the ratio of differences of time differences between any two points on them is constant, and equal to plus or minus one, are plotted on Figures XVI and XVII. When the stations are not in line, it is easy to pick out points between which lorhumb lines do not run and still remain within the limits of station reception, or which first cross the opposite intersection of hyperbolas from that which is desired.



Where solutions are possible, as in most cases, they could well be used in conjunction with a rough great circle course computer to guide the final stage of the approach to the destination. It could be automatically cut in when  $w_d$  and  $y_d$  both fall below a certain limit, to first set up the ratio of  $w_d$  to  $y_d$ , and then transfer control of the autopilot from the first navigation system to the lorhumb computer.



#### IV STREETER AUTOMATIC NAVIGATOR

The Streeter automatic navigator is an analog computer obtaining solutions for latitude, longitude, course, distance to destination, and deviation from desired course while continuously guiding the craft along the desired rhumb line. A block diagram of the system is given in Figure VI. The spherical triangle shown in Figure I(B) is first solved for  $\phi_a$  and  $S_x$  by use of the formulas below:<sup>5</sup>

$$(1) \quad N \sin k_w + N \sin w \cos(\phi - \phi_a) \frac{N}{2} \tan S_x \\ + N \sin \frac{1}{2}(k_w + w) \sin \frac{1}{2}(k_w - w) = 0$$

$$(2) \quad N \sin \frac{1}{2}(k_w + w) N \sin(k_w + w) N \sin \gamma \cos \phi_a \\ - [N \sin k_w + N \sin w \cos(\phi - \phi_a)] [N \sin \frac{(k_y + \gamma)}{2} N \sin \frac{(k_y - \gamma)}{2}] \\ + N \sin \frac{(k_w + w)}{2} N \sin \frac{(k_w - w)}{2} N \sin k_y = 0$$

$$(3) \quad k_y = S_y - S_x$$

$$(4) \quad k_w = S_w - S_x$$

Using these, the latitude and longitude of the position are solved by the formulae:<sup>5</sup>

$$(5) \quad -N \sin(L_r - L_x) + N \sin S_x \cos(\theta + \phi_a) = 0$$

$$(6) \quad -\cos L_r N \sin(\lambda_r - \lambda_x) + N \sin \gamma \sin(\theta + \phi_a) = 0$$



The deviation from the rhumb track is solved by the formula:<sup>5</sup>

$$(7) \quad d = q(\lambda_r - \lambda_d) \cos\left(\frac{L_r - L_d}{2}\right) \cos \tau - q(L_r - L_d)$$

where  $L_r$  and  $\lambda_r$  are the latitude and longitude of the position, and  $L_d$  and  $\lambda_d$ , the latitude and longitude of the destination, and  $q$  is the proportionality constant relating angular and linear measurements on the surface of the earth.

The distance to go is obtained by the formula:<sup>5</sup>

$$(8) \quad S = -q(L_r - L_d) \sec \tau$$

$\tau$  is the angle of the desired track from north.

Multiplication in the system is performed by using the voltage across a potentiometer as the multiplicand, and the percent of the total resistance at the variable tap as the multiplier. The constant  $n$  is introduced in the formulae so that the product of  $n$  and the sine of the limiting magnitude of an arc is equal to unity, since the multiplier must always be less than one. This is because the multiplier is the fraction of the potentiometer across which the output voltage is obtained, and this of course must be less than unity.





## V HYPERBOLIC POSITION RECORDING AND PLOTTING SYSTEMS

Utilizing automatic hyperbolic receivers, systems could be made that would continuously record the position of the craft, without performing the auto-navigation functions. Since a set of hyperbolic coordinates locates position as definitely as other coordinates do, provided the ambiguity of fix is resolved, the simplest method of continuous recording of position would be a tape recording of receiver output. It has also been suggested, that the position could be continuously plotted on a plotting board, with the time differences used as rectangular coordinates. Special charts could be prepared showing the land masses in this coordinate system. The Mass. Inst. of Tech. Radiation Laboratory Series #4, "Loran"<sup>4</sup>, shows on page 111 an illustration of such a chart for the Cape Cod area, still recognizable in its general features. This is particularly feasible for a small area lying entirely on one side of the station base lines. The chart requires the last restriction since for a triplet, a given set of coordinates represents either of two points, so a chart must present area including only one of these points of intersection. Charts such as these distort angular information badly, and would be difficult to use for distance information, as the scales are constantly changing. In figure VIII is shown a chart of this type for the larger area of Newfoundland, demonstrating the distortion occasioned by using the projection over a large area. This would probably make such a system unpopular.



## VI. VECTORIAL ANALOG HYPERBOLIC COURSE COMPUTER

This computer is essentially a homing device, giving continuous guidance between initial position and destination along a great circle course. The input information is: transmitter positions (given in rectangular coordinates with one base line on an axis), and position of destination and continuous position of craft, the last two being given in hyperbolic coordinates. The output of the computer is a signal proportional to the deviation from the desired great circle course, used to correct the course of the craft so as to eliminate the error, and a signal approximately proportional to the distance to the destination, which may be used to initiate some set procedure when a specified distance to travel remains.

The computer obtains the solution for the course and distance to destination vectorially, utilizing the vector qualities of alternating voltages to represent planar vectors from one point to another. The distances and angles between points are represented by voltage magnitudes proportional to the distance, and relative phase equal to the angular displacement. The vector problem is illustrated in Figure VII with the solid lines representing vectors physically generated by phase shifters, and attenuators, and the dotted lines, vectors obtained by vectorial addition of the solid line vectors.

The solution of the problem is obtained in the following manner:



- (1) Station vectors  $XW$  and  $XY$  are set up according to given information of the station positions.
- (2) Hyperbolic coordinates of the destination  $D$  inserted as  $TD_{xy}$  and  $TD_{xw}$ .
- (3) Trial vector  $R_{XD}$  is set into computer as the vector remaining from previous use, or an approximate solution is inserted by hand.
- (4) Vector  $R_{YD}$  is obtained by subtracting  $XY$  from  $R_{XD}$ .
- (5) Vector  $R_{WD}$  is obtained by subtracting  $SW$  from  $R_{XD}$ .
- (6) The magnitudes of  $R_{XD}$ ,  $R_{YD}$ , and  $R_{WD}$  are obtained by rectifiers, and the magnitude of  $R_{XD}$  is subtracted from the magnitudes of  $R_{YD}$  and  $R_{WD}$  to obtain the time differences for the position represented by the assumed vector  $R_{XD}$ .
- (7) The computed time differences are compared to those indicated by the receiver to obtain the time difference errors.
- (8) A servo system, having the time difference errors as an input corrects the vector  $R_{XD}$  till the errors are zero.
- (9) The hyperbolic coordinates of the position are set in by the automatic receiver, and steps 3 to 8 are repeated for the position vector.
- (10) Initial vector  $R_c$  is obtained by subtraction of vector  $R_{XP}$  from  $R_{XD}$ , and reference vector  $R_{cref}$  is made to coincide with it.
- (11) The magnitude of  $R_c$  is given continuously as the distance to go.





(12)  $R_c$  is continuously compared in phase with  $R_{c\text{ref}}$  to give the indication of deviation from the desired course.

(13) The deviation from course output is fed to an autopilot operated to reduce the deviation to zero.

The solution has been obtained in a plane which is a projection of the earth's surface, transformed by location of points according to the oblate spheroidal hyperbolic coordinates on the earth. Each point is transferred to a position on the plane having the same hyperbolic coordinates, with the plane system having the same station separations as the arc separations of the stations on the earth. This type of projection has been found by Robert Frank<sup>1</sup> to correspond closely to a gnomonic projection for most station configurations. The gnomonic projection plane is located so that the stations project on the plane with separations equaling the arc separations on the earth. A gnomonic projection is one for which points are projected by passing a radius from the center of the earth through the point and using the intersection of the radius with the plane as the transformed point. Due to this projection system, all great circles project as straight lines. Therefore, if the craft is guided so that the phase of  $R_c$  remains constant, it will follow a straight line in the plane which will project as a great circle on the earth.





In Figure XXIV for rates 1L3 and 1L4, the Greenland, Labrador, and Newfoundland loran triplet are plotted plane hyperbolas with station separations equal to arc separation of the stations on the earth. Four great circles were selected, the meridians  $35^{\circ}\text{W}$ ,  $45^{\circ}\text{W}$ , and  $65^{\circ}\text{W}$ , and the base line extension for rate 1L2. At selected points along these great circles as found plotted on a standard loran chart for the area, the loran coordinates were obtained. By construction, these coordinates were plotted on the plane, and their intersection shown as the small circles in Figure XXIV. The accuracy of construction was such that the intersection of the coordinate hyperbolas lies within the circles. Straight lines were then drawn as dashed lines through the extreme points. The great circles projected as straight lines within the construction accuracy.

The relationship between the distance remaining to be covered as plotted on the plane and this distance projected onto the earth is rather complex. However, conversion from one projection to the other could be made by reference to a series of graphs drawn for each station group to be used, each graph being drawn for one value of magnitude  $R_{XD}$ , and having a curve of correction factors given for coordinates  $R_{XP}$  along with the angle between position and destination vectors. Being a homing system primarily, accurate knowledge of distance left to travel is not necessary. Assurance that the craft is being properly navigated may be had by location of position in hyperbolic coordinates on a map of the region



## VII CHOICE OF A SYSTEM FOR CONSTRUCTION

The previous systems are several of those which might be used in automatic hyperbolic navigation. The vectorial analog computer last described was decided upon as the simplest to use as an accurate enough homing device following a reasonable approach to a great circle. The computer seems easiest to build to the required accuracy without encountering the bulk of the digital computer. It was the system which seemed least apt to fail to reach the destination assuming reasonable system errors, and changes that might occur while enroute. Utilizing the vector properties of alternating voltages, the system should be simpler than a system that operated on a rectangular coordinate basis, with the necessity of resolving voltages into quadrature components extremely accurately and sufficiently stable. A rectangular system would also call for a mechanical or electrical conversion of shaft rotations into sines of the angles of rotation.

The remainder of this paper will be devoted to a description of the adopted system, as put into realization at Sperry Gyroscope Company.



## VIII CIRCUIT DESCRIPTION OF VECTOR COMPUTER

A block diagram of the vector analog hyperbolic course computer is shown in Figure IX. A description of the individual blocks of this diagram will be given in this chapter. The subscripts P and D are used to denote use for Position and Destination respectively. A vector or voltage used for either is generalized by dropping these subscripts.

### 1. Oscillator:

The 1000 cycle per second oscillator supplies through a common transformer, the reference voltage  $E_{ref}$ , to all other units. The Oscillator, shown in Figure X, is a Wien bridge type oscillator, amplitude stabilized by the use of a Western Electric 1A thermistor as the resistance in one arm of the frequency determining bridge. By employing six 6AQ5 tubes in push-pull for the output stage, and using degenerative feedback from the secondary side of the output transformer, 20 watts is supplied to the system with less than .2% harmonic distortion.

### 2. Phase Shifter Chassis:

The phase shifter chassis, shown in Figure XI, provides the voltages  $R_{cref}$ ,  $R_{XP}$ ,  $R_{XD}$ ,  $T_{XP}$ , and  $T_{XD}$ . The first three of these voltages have their phases varied by two phase synchro resolvers, with the phase shift equal to the mechanical rotation of the rotor shaft. The magnitudes of  $R_{XD}$ , and  $R_{XP}$  are varied by linear ten turn helipot resistor attenuators, which have increments of resistance small enough to maintain the desired voltage resolution of the system.





When the system is operated to correct voltage  $R_{XD}$  to concur with the hyperbolic coordinates of the destination, the output of the  $R_{XP}$  potentiometer is grounded, the variable tap of the  $R_{XD}$  potentiometer is grounded, and the  $R_{XD}$  voltage is taken from one end of the potentiometer. In this operation, the  $R_X$  isolation amplifier is a load across the  $R_{XD}$  potentiometer output. When the computer is operated to compute the position and course vectors, the  $R_X$  isolation amplifier is switched to the variable tap of the  $R_{XP}$  potentiometer, and the end of the potentiometer is connected to the variable tap of the  $R_{XP}$  potentiometer. Then, from ground to the center tap we have the vector addition of  $R_{XP}$  and the negative of  $R_{XD}$  to form  $R_C$ , which is connected to its isolation amplifier for further use without interaction on the previous networks. Since it is important that  $R_{XD}$  not change after it is computed, and the loads on it are changed during the computation of  $R_{XP}$  and  $R_C$ ,  $R_{DL}$  and  $C_{DL}$  are connected as a load on  $R_{XD}$  to maintain a constant total load impedance. The potentiometers  $T_{XP}$  and  $T_{XD}$  are geared to potentiometers  $R_{XP}$  and  $R_{XD}$  respectively and supplied by the reference voltage  $E_{ref}$  to give the same magnitude (or slightly greater) voltages as  $R_{XP}$  and  $R_{XD}$ . Their outputs are used so that all the processes of detection and subtraction to obtain  $R_X$ ,  $R_Y$ , and  $R_W$  are repeated at about the same level with the time difference inputs from the hyperbolic system receiver, to reduce system non-linearities of detection, and to provide a convenient means of obtaining time difference error for the assumed  $R_X$ .





### 3. Time Difference and Station Base Chassis:

In the time difference and station base chassis shown in Figure XII, the loran coordinates of the destination and position are inserted as shaft rotations proportional to time differences. These time differences have coding delays removed through a differential coding delay input, so that the time difference used by the computer for points equal distance from stations has a value of zero. The time difference inputs vary taps on 15 turn .02% linear helipot to give a voltage between it and the center tap of the balanced input proportional to time difference, with positive phase voltages representing time differences towards the master station, and negative phase voltages differences on the slave station side of the line of zero time difference. These voltages are in phase with  $E_{ref}$ , and are connected in series with the voltage  $T_X$  assumed to be the time separation of P (or D) from X, to give the magnitudes of time separation of P (or D) from Y and W,  $T_Y$  and  $T_W$  respectively, since  $T_Y$  is equal to the sum of  $T_X$  and  $TD_{XY}$ , and  $T_W$  is the sum of  $T_X$  and  $TD_{XW}$ . Error in assumption of  $T_X$  is later cancelled by subtracting the magnitude of  $T_X$  from the magnitudes of  $T_Y$  and  $T_W$  to again obtain the magnitudes of  $TD_{XY}$  and  $TD_{XW}$  as DC voltages of proper polarity, and with the new values of time differences affected by system nonlinearities to approximately the same extent as were the computed space differences for the assumed  $R_X$  vector, since they were used at the same



levels in detection and subtraction, in similar circuits.

To protect the homing accuracy of the system without increasing the demand for linearity of time difference potentiometers, for both position and destination the time difference voltages are obtained from the same .02% linear helipots. After the destination vector is computed, using these time difference helipots, the time difference voltage output is switched to a set of reference helipots, having the same voltage resolution, but having no stringent linearity requirements. These helipots are then adjusted to agree with the destination vector as determined by zero indication on time difference error meters. This then preserves the destination time differences voltages for further use without disturbing the main time difference helipots. The voltages may be used to recompute the destination vector during flight to correct any drift in that vector. The object of the computer, then, is to guide the craft to the point where the voltages on the main time difference potentiometers are the same as those originally set on them for the coordinates of the destination. Being able to reset the destination vector several times during the flight enhances the accuracy of performing this, since if the destination vector has not shifted, the main potentiometers are at the destination time differences when the position and destination vectors are coincident.

The station vectors are generated by a rectangular coordinate system, in which the station vector XW is represented





by the voltage  $B_W$ , in the phase with  $E_{ref}$ . The vector  $XY$  is obtained by the vector addition of its rectangular components parallel to  $E_{ref}$  and components perpendicular to  $E_{ref}$ , represented by voltages  $B_Y$  and  $B_X$  respectively. A loaded RC network across a balanced voltage source is used to obtain the quadrature voltage  $B_X$ , whose magnitude is varied by varying the tap distance from the transformer center tap on the  $B_X$  helipot. The vector additions of  $B_X$ ,  $B_Y$ , and  $R_X$  indicated in Figure VII is performed by connecting  $R_X$  to the helipot  $B_X$  tap.  $R_X$  is obtained from a low impedance source, so the voltage at this point is not affected by the remainder of the circuit. To represent the circuit as seen at the  $R_Y$  detector input, Thevenin's theorem may be used, and is represented as an equivalent voltage source and an equivalent series impedance with detector  $R_Y$  as its load. The equivalent voltage is equal to the voltage at the input with no load. Since the only ground connections of the network are through the  $R_Y$  detector and through the source of  $R_X$ , if the detector input is open circuited, no current can flow through the  $R_X$  source. Since this is true, the equivalent Thevenin's voltage is equal to voltage  $R_X$  plus a voltage independent of the voltage  $R_X$ . The equivalent Thevenin impedance is equal to the impedance at the detector input with the voltage sources shorted, so this too, is independent of  $R_X$ . The detector equivalent input voltage then, is  $R_X - B_X - B_Y = R_Y$  in series with the equivalent impedance. To keep this



by the voltage  $B_W$ , in the phase with  $E_{ref}$ . The vector XY is obtained by the vector addition of its rectangular components parallel to  $E_{ref}$  and components perpendicular to  $E_{ref}$ , represented by voltages  $B_Y$  and  $B_X$  respectively. A loaded RC network across a balanced voltage source is used to obtain the quadrature voltage  $B_X$ , whose magnitude is varied by varying the tap distance from the transformer center tap on the  $B_X$  helipot. The vector additions of  $B_X$ ,  $B_Y$ , and  $R_X$  indicated in Figure VII is performed by connecting  $R_X$  to the helipot  $B_X$  tap.  $R_X$  is obtained from a low impedance source, so the voltage at this point is not affected by the remainder of the circuit. To represent the circuit as seen at the  $R_Y$  detector input, Thevenin's theorem may be used, and is represented as an equivalent voltage source and an equivalent series impedance with detector  $R_Y$  as its load. The equivalent voltage is equal to the voltage at the input with no load. Since the only ground connections of the network are through the  $R_Y$  detector and through the source of  $R_X$ , if the detector input is open circuited, no current can flow through the  $R_X$  source. Since this is true, the equivalent Thevenin's voltage is equal to voltage  $R_X$  plus a voltage independent of the voltage  $R_X$ . The equivalent Thevenin impedance is equal to the impedance at the detector input with the voltage sources shorted, so this too, is independent of  $R_X$ . The detector equivalent input voltage then, is  $R_X - B_X - B_Y = R_Y$  in series with the equivalent impedance. To keep this





impedance constant,  $R_{CY}$  is geared to  $B_Y$ , and kept of the proper magnitude to keep the impedance at the input of the detector independent of the position of the  $B_Y$  tap.  $R_{CX}$  is geared to  $B_X$  helipot to keep the impedance independent of the  $B_X$  tap.  $R_X$  is directly connected to its detector, since its source impedance effectively does not vary,  $R_W$  is connected to its detector in series with  $R_{CW}$ , which is geared to  $B_W$  so as to keep the magnitude of its source impedance to the detector constant. Also, to load the balanced supply for the station network symmetrically, and to insure that the full scale voltages on pots  $B_Y$  and the corresponding resistor in the opposite side of the network, remain equal, when  $R$  is adjusted to make  $B_X$  accurately in quadrature with  $E_{ref}$ , a similar network is added, consisting of  $C_A$ ,  $R_C$ ,  $R_D$ , and  $R_B$ . The latter resistor is varied by the same shaft as  $R_A$ , to keep the resistance arms equal, and thus keep the loads balanced.

#### 4. Isolation Amplifiers:

All outputs of the phase shifter chassis are made through isolation amplifiers to isolate the effects of their loads from other parts of the system, and so that the output impedances of the voltages will be low to allow series addition of voltages with the source impedances contributing a negligible effect. These amplifiers, shown in Figure XIII, are RC coupled amplifiers with a push-pull transformer coupled output. The amplifiers have internal gain of about 6,600, and utilize negative feedback from the secondary side



of the output transformer to give a gain of from 1 to 12.

#### 5. Detector Sub Chassis:

The output voltages representing the assumed vectors from the stations to P (or D), and the assumed time separations of the stations and P (or D) are rectified in detectors and combined in the circuit shown in Figure XIV to produce the time difference errors of the assumed position. These detectors suppress even harmonics by their push-pull arrangement as a voltage doubler having an unbalanced input. The values of resistances in the circuits are proportioned so that the diodes conduct for one third of a cycle of the 1000 cycle voltage. Since the detectors are average reading, whole cycles of harmonics produce no output. Therefore, the third harmonic and integral multiples of the third harmonic produce no effect on the output. This leaves the fifth and seventh harmonics not especially suppressed, for they have other than an integral number of cycles during the conduction of the diodes. However, in an average reading detector, the only effect of these harmonics is that due to the residue over an integral number of cycles. The fifth and seventh harmonics producing the worse effects are overcome by holding these harmonics down in the remainder of the circuits to a value that will cause no appreciable error. Up to this point, all voltage additions were made, and operations carried out in linear elements, so that harmonics may still be separated from the fundamental, leaving the value that would have existed with no harmonics.





To maintain the high input impedances to the detector, and high impedances in its output side, the detectors will each be hermetically sealed in a plug-in unit. No moving parts will be required within the sealed unit. Hermetic sealing is necessary to stop changes in resistances due to the effect of changing humidity and dust upon leakage. Diodes should be chosen that have back resistance of greater than 6000 megohms, so that this leakage if it changes slightly will not affect the accuracy of the system. Such diodes may be obtained by selection from standard diodes. Of some 20 6AL5 diodes measured, all but 5 tube halves had back resistances ranging from 40,000 to over 200,000 megohms, the other 5 tubes being unsatisfactory.

Each detector has a variable DC voltage in series with it, impressed across a low resistance, adjustable so that the contact potentials of all diodes may be equalized, and the error output with zero input to all detectors will be zero. In series with the input of each detector is a variable resistor of large enough value so that the current sensitivities of all the detectors can be made equal.

Any increase in the source impedance of a detector, by voltage divider effect with the input impedance of the detector, will decrease the detector voltage output. The source impedances of  $T_W$  and  $T_Y$ , as an example, change as shown in the simplified diagram shown in Figure I(B). The source impedance change of  $T_X$ , coming from its isolation amplifier, may be neglected. The source impedance, then,





is approximately  $R_1$  in parallel with  $R_2$ , neglecting the source impedance of the transformer. This source impedance produces a change of voltage output, but may be compensated for by inserting in the detector load an impedance which varies inversely with the source impedance, and of a magnitude to keep the current sensitivity constant. For this purpose,  $R_{CW}$ , on the time difference chassis, is geared to the  $TD_{XW}$  helipot, and  $R_{CY}$  to the  $TD_{XY}$  helipot.

Detectors  $R_Y$  and  $R_W$  maintain constant current sensitivity by the addition of compensation resistors  $R_{CX}$ ,  $R_{CY}$ , and  $R_{CW}$  in series with their inputs (resistors are located on station base chassis shown in Figure XII and geared to helipots  $B_X$ ,  $B_Y$ , and  $B_W$ ). Their magnitudes are varied so that the source impedance to the detectors will appear constant.

The detector outputs, then, are proportional to the magnitudes of the fundamental components of the input voltage, independent of change of source impedances. Their outputs are arranged in two groups so that the resultant two voltages will be proportional to the error in time differences for the assumed position. The additions made are:

$$(1) \quad R_Y - R_X + T_X - T_Y = \text{error in } TD_{XY}$$

$$(2) \quad R_W - R_X + T_X - T_W = \text{error in } TD_{XW}$$

The voltages may be thought of as being added by adding the currents they cause to flow in a low common resistance. Since the output impedances are large, the interaction



between circuits is negligible. When the time difference error is zero, the currents exactly add up to zero. At balanced conditions, the balance would not be disturbed by opening the mixing resistor, so this is done in this circuit, merely tying the detector outputs to a common bus for each group. When the time differences are incorrect, the voltage is connected to one side of a vibrator, the other side of which is grounded.

#### 6. Servo Amplifier:

The movable contact on the vibrator is made to connect first to the detector output bus, and then to ground potential at a 400 cycle rate. The voltage on the movable contact, then, is a square wave whose magnitude is proportional to the time difference error, and is connected to the grid of a paraphase amplifier. The vibrator is used to convert the DC error signal to an AC signal, which may be amplified stably, avoiding the unstability of DC amplifiers whose "zero" level must remain fixed. The sign of the DC error is preserved by the phase relationship between the square wave and the 400 cycle supply that drives the vibrator. The square wave is amplified, as shown in Figure XV, in an amplifier stage, and in a paraphase amplifier, whose output is used to drive the grids of the phase sensitive demodulator stage with the square waves of opposite phase. The 400 cycle sinewave that drives the vibrator is applied to the plates of these tubes. This sinewave is in phase with one of the grids, and out of phase with the other grid,





with phase reversal of the grids taking place when the DC error signal changes sign. With balanced conditions, the square wave input to both tubes is zero, so both conduct for the same length of time when their plates are positive, thereby making their cathodes have the same average voltage. When the error square wave increases, one grid is more positive than the other during the conduction portion of the cycle. Therefore, one cathode becomes more positive than the other, and the output signal taken as the voltage between the two cathodes is a DC voltage that is equal to the error DC input voltage amplified, maintaining the sign of the error.

Two systems of accomplishing the correction of  $R_X$  are available so that the differences of  $R_X$ ,  $R_Y$ , and  $R_W$  will agree with the time differences of the position as given by the receiver. In one method the error in  $TD_{XY}$  is used to correct the phase of  $R_X$  and the error in  $TD_{XW}$  is used to correct the magnitude of  $R_X$  by rotation of the position phase shifter and attenuator respectively. For a situation such as exists in Figure I(C) the sensitivity of correction is poor. However, if the time difference errors were used in the reverse order to make the corrections to  $R_X$ , the sensitivity would be much better. Making the computer sensitive as to which way the time difference errors should be used for best sensitivity would be difficult, so a second system of correction is available. In this system, the error in the differences of time differences is used to correct the



phase of  $R_X$ , and the error in the sums of time differences is used to correct the magnitude of  $R_X$ . These errors may be obtained by the addition and subtraction of the errors of time differences as this is a linear system. This is accomplished by switching the outputs of the paraphase amplifiers to add or subtract in common resistors. This system approaches the sensitivity of an  $R, \theta$  system for many station configurations, and therefore, the sensitivity remains about constant at any place in the plane. The areas of least sensitivity lie along the base line extensions, where the sensitivity of the hyperbolic system itself is poor. Illustrations of the loci of sums and differences of time differences for two station configurations are shown in Figures XVI, and XVII. These are typical configurations, and the loci approximate an  $R, \theta$  coordinate system.

Both systems of correcting the  $R_X$  vector may be shown to converge on the correct position for any point on the plane. However, there are two intersections of time difference hyperbolas, either of which the computer could accept as correct unless instructed as to which side of the station bases the desired solution lies. This instruction is set in by means of the servo system used to correct the phase of  $R_X$  by setting the direction of phase correction for positive time difference errors. Having the sensing of the phase servo system set, the computer will always seek out the solution on one side of the station bases. For the solution on the other side of the stations, the sensing must be reversed.





In case of a solution lying beyond the extreme radius of the computer, the phase servo sets in about the correct angle, and the magnitude servo runs out to its largest value and is stopped by a limit switch.

#### 7. Phase Detector:

The voltage representing  $R_C$  is connected to the center tap of the secondary of the output transformer of the course reference isolation amplifier. The balanced terminals of the secondary are the inputs of the phase detector shown in Figure XVIII. This phase detector consists of two harmonic suppressing detectors similar to the other detectors used, but using 6X4 diodes to accomodate the larger maximum voltages encountered, and using a different load configuration using voltage rather than current output. The outputs of the two detectors will differ by approximately the product of the phase difference between  $R_C$  and  $R_{Cref}$  expressed in radians and the magnitude of  $R_C$  as long as  $R_{Cref}$  remains large compared to  $R_C$ , and the phase difference is small. It is to be noted that the voltage representing  $R_{Cref}$  is in quadrature with that vector. The outputs of the phase detectors are connected to the contacts of a vibrator. Therefore, the voltage applied by the movable contact of the vibrator to the servo amplifier is a 400 cycle square wave whose amplitude is proportional to the distance of deviation from the desired track. To insure that the error output will be zero at the destination, and all points along the desired track, the output transformer for  $R_{Cref}$  must be accurately balanced. This is done by careful construction of two similar windings on



a common core, and obtaining the center tap by applying  $R_c$  to a variable tap on a resistor connected to points a few turns in from the common connection of both coils.



## IX PREDICTED EFFECTS OF SYSTEM ERRORS

### 1. Phase Shift in $R_{Cref}$ .

If the phase of  $R_{Cref}$  shifts after its initial setting, the phase detector will show a deviation from the course, so the autopilot will act to eliminate this error output, and the craft will follow the new vector to the destination. A continuously changing phase of  $R_{Cref}$  will cause the track to be curved, as illustrated in Figure XX(A).

### 2. Phase Shift in $R_C$ .

If, in the vector addition of  $R_P$  and  $R_D$  to obtain  $R_C$  there is a phase shift in any of the voltages after setting up the course reference voltage, the phase detector will show an error voltage, which the autopilot will attempt to correct to zero. The path followed is curved as shown in Figure XX(B) so that at all times, the course voltage when shifted, will have the phase of the initial course voltage. If the phase shift occurs at the start of the problem, then  $R_{Cref}$  will be set up incorrectly by the angle of the phase shift, and the  $R_C$  voltage, also having this shift, will be in phase with it, so the phase detector will show zero error, and a straight, correct course will be followed, providing the phase shift remains constant. If, however, it changes with the decreasing level of  $R_C$ , the course will be curved similar to the result of a phase shift in  $R_C$  after setting  $R_{Cref}$  as shown in Figure XX(B)

### 3. Effect of an unbalance of Phase Detector or course servo.

If, during the problem, there is this type of unbalance,





caused by an unbalanced  $R_{Cref}$  output transformer, unbalance in the servo paraphase amplifier, or in the phase sensitive demodulator, the error will be reduced to zero by flying off the desired course until the unbalance is offset by a course error. The output of the phase detector is proportional to distance off course, so this distance will be maintained about constant as shown in Figure XX(C), and this will be the closest approach made to the destination.

#### 4. Effect of non-intersection of hyperbolas.

Due to incorrect station information, or inherent faults in utilizing plane hyperbolas rather than oblate spheroidal hyperbolas, a point on the earth may be passed through for which the time difference coordinates on the plane corresponding to those on the earth do not have an intersection. This is illustrated in Figure XXI. The problem first proceeds normally, with the path being constrained to points of intersection of hyperbolas which lie along the initial course vector. A little further, there is no intersection of the hyperbolas obtained from the receiver for the position of the craft. In trying to find the intersection, the phase of  $R_X$  will be held about correct, and the magnitude changed to its maximum value (or to zero) as shown in Figure XXI. The course voltage then will be out of phase with  $R_{Cref}$ , and to correct this indicated error, the craft's course is changed to be about parallel to the  $R_C$  vector, until the time differences from the receiver again have an intersection on the plane. The  $R_X$  vector will then correspond to this intersection,



which will lie off the desired course due to the previous attempt to bring  $R_c$  in phase with  $R_{c\text{ref}}$ .  $R_c$  will now be out of phase with its reference voltage, and the servo system will eliminate this error, and follow the desired track from then till the destination is reached.

#### 5. Effect of error in station Base vectors.

Due to phase shift of the  $B_X$  quadrature voltage, incorrect calibration of helipots, or setting of the voltages in these helipots, the station vectors may be given the computer in error. This may result in deviation from a straight line course on the plane for the reasons shown in the previous case. Apart from deviations in the track as seen by the computer in case (4), the track will differ from a straight line in the plane. An illustration of an extreme error of 30 degrees in the angle between station bases is shown in Figure XXII. Intersections of the plane hyperbolas for the correct station vectors, corresponding to those in the plane for the station vectors seen by the computer, show the actual path followed in the plane. As shown, it is curved, so the path projected on the earth will depart from a great circle, but the craft will still reach the destination.

#### 6. Effect of nonlinearities of detectors.

If the detectors have different, but constant characteristics, the voltages representing  $R_p$  and  $R_D$  to obtain the time differences corresponding to their position will be incorrect. However, since the same amplifiers, time difference potentiometers, and detectors are used to obtain both the



position and destination vectors, the craft will be guided in the plane until  $R_P$  coincides with  $R_D$ , at which time all variables will be identical for both vectors, so the time difference helipots will be at the same point, and therefore, the craft will be at the destination. A curved course will be followed, however, as the scale of time differences obtained by subtracting the position vectors will vary. If the characteristics of the detectors change during the problem, as by change in diode contact potentials, or changed sensitivities due to change in resistance values or leakages, the vector  $R_P$  will coincide with the vector  $R_D$  for time differences not those of the destination. A differential change of detector outputs of about .013 volts will cause a one microsecond error of final position.





## X LABORATORY TESTS OF COMPUTER

### 1. Oscillator.

The first type oscillator tried utilized a mazda bulb in the opposite resistance arm from that in which the Western Electric Thermistor is now placed. This type of amplitude stabilization is unsatisfactory for any equipment subject to vibration. Just the vibration occurring in the laboratory caused the output level to change enough to make the computer inoperative. The Thermistor amplitude stabilizer was found to be quite satisfactory. By the use of negative temperature coefficient capacitors, and resistors of the opposite temperature coefficient, the frequency stability was adequate for laboratory operation. Further tests may show that the unit should be roughly temperature controlled within a region of ten degrees for air operation. Harmonic content of the oscillator, with full load, was as indicated below:

2nd harmonic	-----	.15%
3rd harmonic	-----	.45%
4th harmonic	-----	.000%
5th harmonic	-----	.055%
6th harmonic	-----	.000%
7th harmonic	-----	.01%

### 2. Phase Shifter Chassis.

The item of particular interest on this chassis is the synchro phase shifter. Linearity of phase shift with shaft rotation is not particularly important to this computer since the shaft angles are not measured in the process of solution.



Of importance however, is stability of phase shift, since the phase of the destination vector is considered constant after each computation of that vector. In this respect, the phase shifters were not a great success, since the phase varied more than desirable for changes in input voltages. This requires utmost amplitude stability of the oscillator. Also, rotating the synchros caused interaction on the other synchros, by changing the load on the common transformer winding, thereby changing the phase output of the synchros. This effect was noted to cause a phase shift of about 0.03 degrees for a change of load on a winding of one percent. For the position and destination, this would cause errors up to one or two microseconds.

The phase shifters also introduced considerable harmonics, and were measured to multiply the input harmonics of the oscillator by a factor of three or four.

### 3. Time difference and station base chassis.

Originally, it was planned to obtain the vector  $R_W$  from the opposite half of the balanced transformer, from which  $R_Y$  is obtained. This is shown in Figure XII as  $R_{W1}$ . However, the detector load of this vector caused interaction with the other vector as the  $B_W$  helipot was varied. This was due to the flow of detector currents through a common resistance,  $B_X$ . To overcome this, the  $B_W$  helipot was provided with a separate transformer winding, and the station vector  $XW$  was made to be composed solely of an in phase voltage, rather than using quadrature components in both station vectors as pre-



viously planned. With the quadrature voltage available, this increased the minimum angle available between station bases.

The methods used for compensation of changes in source impedances to detectors occurring on this chassis was changed from that shown in Figure XII. The revised method called for operating the detectors for  $T_X$  and  $R_X$  separately, and paired with the other time and vector detectors. The  $T_X$  detectors have in series with their inputs, compensation resistances identical to the  $TD_{XW}$ , and  $TD_{XY}$  helipot impedances presented to the  $T_W$  and  $T_Y$  detectors. The compensation potentiometers are geared to the time difference helipots whose source impedance they repeat. By this means the input impedances to a pair of detectors are kept identical, so that their sensitivities will be the same. A similar compensation system is also used for the station base network, by introducing identical impedances in the  $R_X$  detectors as introduced by the sources of the  $R_W$  and  $R_Y$  detectors. For this purpose, compensation impedances are placed in series with the  $R_X$  detector inputs, and geared to  $B_X$ ,  $B_Y$ , and  $B_W$ .





#### 4. Isolation Amplifiers.

The isolation amplifiers were found to have internal gains of 6,600 to 7,000, and to have output impedances of about 5 ohms. They introduced no measurable harmonic distortion for inputs less than 200 volts. The  $T_X$  isolation amplifier was adjusted to have an accurate gain of unity at full voltage input, and the input and the output were compared by use of the detectors and servo systems, as the input was decreased to zero. The gain introduced no unbalance in the detector voltages other than that due to lack of tracking of detectors (about .05 volt differential output).

#### 5. Detector sub-chassis.

The detector arrangement first tried was that shown in Figure XIX, in which only one detector was used for each  $R_X$ , and  $T_X$ . The equations used at balanced conditions are:

$$(1) \quad R_W = R_X - T_X + T_W$$

$$(2) \quad R_Y = R_X - T_X + T_Y$$

For these equations,  $R_X - T_X$  is common to both equations, and is the voltage on the 1 microfarad capacitor, and is about equal to zero, since the two voltages are made approximately equal. The system fell down first due to 1,000 cycle voltages across the common capacitor causing interaction. This was overcome by connecting the low sides of the detectors to the common point by filter sections. This was successful in removing the interaction due to the 1,000 cycle voltage. However, the leakage from the high side of the detectors to ground, and the resistance from the common bus to ground



formed a voltage divider across the detector voltage, impressing a DC voltage of about 0.1% on the common bus which raised the other detector levels causing interactions and false balances. For these reasons, the detector arrangement shown in Figure XIV was adopted.

One of the limiting factors in the computer will be the variation of diode contact potentials after making the balancing adjustment for them. They were observed to cause an unbalance equal to a two microsecond time difference error over a period of several hours. However, some diodes changed contact potential by as much as a ten microsecond error when subject to vibration. Sensitivities of the detectors also required resetting each time the computer was turned on. After adjusting contact potentials and sensitivities, two detectors with the same voltage inputs would track as the voltage was varied from zero to two hundred volts with an unbalance less than that caused by a half microsecond time difference error. The time constants of the detectors must be watched closely so that a varying oscillator voltage will not cause a varying error voltage. Variations of balance due to this effect were held down to the extent that modulating the 1,000 cycle input to two detectors by 50% at a rate of one cycle per two seconds caused a time difference error of plus or minus one microsecond.

The suppression of harmonics was very good. To cause a one microsecond error of time difference reading, tests showed that 3% of 2nd, 3rd, and 6th harmonics must be present. The same error would be caused by 0.7% 5th harmonic.



## 6. Servo Amplifier.

The servo amplifiers were quite satisfactory, though a second stage of amplification and a power stage would be needed for motor control. It is possible that a magnetic amplifier would prove valuable for use here due to its stability. The balance of this servo system with zero input remained constant over a period of several weeks with less error than that caused by a half microsecond time difference error. The early stages require good shielding to prevent pickup from the vibrator supply.

## 7. Phase detector.

The phase detector proved adequately stable and sensitive. A 0.003 degree change in phase was detectable as an output error voltage of 0.6 volts. The drift of the system over a three hour period is about equal to .02 degrees phase shift, and this could be lessened by further work on this unit.

## 8. System performance.

As a means of checking compensations, and making calibration curves, the use of station base line extensions is invaluable. (These are located by changing the phase of the position vector while varying the time difference helipots to keep the time difference errors zero, until the time differences are minimum if on the side of the slave station, or maximum if on the side of the master station). When the detectors track, any change in time differences as the position vector is increased or decreased is minimized by adjust-







ment of the compensation resistors. Calibration of these resistors is made by noting the setting for various positions of the station base helipots. Using this technique the base line extension changed value by 3 microseconds as the position vector varied from maximum to the slave station value. The values of the voltages of the station bases changed scale slightly as the various helipots were changed and the quadrature component changed phase. Compensating for the phase change produced a further scale change. However, calibration of the potentiometer settings may be made by checking the base line extension values and adjusting them to be correct. Then using only  $R_Y$  and  $R_W$ , and a corresponding change in detector inputs, the base line extension for stations Y and W is found. The quadrature component for the Y base line is then adjusted so that this value is correct. The base line extension for XY is then corrected and the procedure repeated until all three are in agreement with the actual station separations.

Plotted in Figure XXIII is a track computed in a preliminary test for a case in which the stations are in line, and station separations were equal. Deviation from a straight line in the plane was ten miles or less. The track was run by the following procedure. First the coordinates of the destination were set in, and  $R_{XD}$  adjusted for zero time difference error. Second  $R_{XP}$  was set, and  $R_{Cref}$  was set for zero phase detector error. Then  $TD_{XW}$  was changed, and  $TD_{XY}$ , and  $R_{XP}$  adjusted until the time difference errors, and phase



detector errors were all zero. The time differences were then noted and plotted as the position  $P_1$ . This was repeated several times until the destination was reached. The distance travelled was 1200 miles, and the destination was approached within less than .7 miles.

In Appendix B is recorded the loran coordinates of fixes on tracks run, and the deviation from a great circle track obtained from a loran chart of the area. The tracks were quite satisfactory, involving about 0.1% excess travel. A 5% error set into one station base did not cause over 0.5% excess travel.



## XI CONCLUSION

Tests on the system up to this time showed no indication of any part of the system failing to the extent that accuracy of 10 microseconds could not be achieved. With change of the phase shifters presently used to capacity phase shifters, and other minor changes, the system could probably be made accurate to within 2 microseconds. Change of detector sensitivities and diode contact potentials will probably require adjustment of these quantities each time the equipment is turned on, and twice daily thereafter.

The equipment could probably be packaged in a chassis of 10 or 12 cubic feet, or less, be accurate to 10 microseconds fairly easily, and to 2 microseconds out of 15,000 microseconds by making precise and frequent calibrations and corrections, without circuit or component changes. By a thorough miniaturization and component stabilization study, the size could be greatly decreased, and the system made accurate to 2 microseconds out of 15,000 microseconds with daily calibration.

Primarily the system is designed for aircraft use, and attempts to extend it to use on ships or requiring an indication of position in terms of latitude and longitude, or requiring a latitude and longitude continuous plot would probably necessitate a different, more complex system.





## APPENDIX A

In this appendix is included data on nine lorhumb tracks plotted on a standard loran chart for the Newfoundland, Greenland, Iceland area.

### Case 1.

This case was plotted for a loran triplet comprised of rates 1-L-5 and 1-L-6, and compared to a great circle between the two points  $P_0$  and D, separated by 480 miles. The positions of the points in latitude and longitude are:

$P_0$	latitude	$55^{\circ}\text{N}$
	longitude	$10^{\circ} 45'\text{W}$
D	latitude	$63^{\circ} 00'\text{N}$
	longitude	$10^{\circ} 45'\text{W}$

The greatest deviation from a great circle was 10% of the path length, or 50 miles. The percent excess travel was 5.2%, or 25 miles.

### Case 2.

This case was also plotted for the loran triplet comprising rates 1-L-5 and 1-L-6 between the points:

$P_0$	latitude	$49^{\circ} 17'\text{N}$
	longitude	$14^{\circ} 30'\text{W}$
D	latitude	$63^{\circ} 38'\text{N}$
	longitude	$14^{\circ} 30'\text{W}$

Path length --- 861 miles

Deviation from great circle -- 30 miles, or 3.5%

Excess travel --- 7 miles, or 0.8%



### Case 3.

This case was plotted for the loran triplet comprising rates 1-L-3 and 1-L-4 between the following points with the results indicated:

P<sub>0</sub> latitude ----- 59° 20' N  
longitude ----- 40° 25' W

D latitude ----- 40° 40' N  
longitude ----- 40° 25' W

Great circle path length ---- 2000 miles.

Deviation from great circle ---- 180 miles --9%

Excess travel ----- 85 miles --4.25%

### Case 4.

This case utilized the same great circle route and points of departure and destination. Two loran pairs were used, comprising rates 1-L-3 and 1-L-5, whose station base lines are about parallel. The lorhumb line did not reach the destination, as when it approached hyperbolas 1-L-3-1900 and 1-L-5-1200, these hyperbolas are parallel, and the track went at right angles to the great circle, and sought the alternate solution for the intersection of the destination hyperbolas, which was beyond reception range of one pair.

### Case 5.

This case was plotted for the same points as cases 3 and 4, using rates 1-L-3 and 1-L-6, for which the hyperbolas 1-L-3-2100 and 1-L-6-2220 are parallel along the great circle. Again when nearing these lines, the track deviated greatly and sought out the alternate intersection of the destination



hyperbolas, which was beyond range of reception of one pair.

#### Case 6.

This case utilized two pairs comprising rates 1-L-5 and 1-L-4. Between the points:

P <sub>0</sub>	latitude -----	53° 00' N
	longitude -----	30° 00' W
D	latitude -----	62° 32' N
	longitude -----	30° 00' W

Lines 1-L-5-1050 and 1-L-4-8150 are parallel where they cross the great circle, and again the lorhumb track deviated greatly and did not reach the destination.

#### Case 7.

This case utilized the same station pairs as Case 6, the same departure point, P<sub>0</sub>, but with a destination of the same great circle just short of the point where the parallel lines crossed the great circle. The destination and results were as below:

D	latitude -----	61° 17' N
	longitude -----	30° 00' W

Great circle path length --- 497 miles

Deviation from great circle -- 75 miles -- 15%

Excess travel ----- 57 miles ---- 12%

#### Case 8.

This case was plotted for the loran triplet comprising rates 1-L-4 and 1-L-3. The lines 1-L-4-8230 and 1-L-3-1410 are parallel where they cross the great circle path to be travelled. The points of departure and destination are:

P <sub>0</sub>	latitude -----	62° 37' N
	longitude -----	53° 30' W
D	latitude -----	64° 10' N
	longitude -----	36° 30' W





The lorhumb line for this case deviated by 235 miles from the great circle course, at which point it reached the alternate intersection of the destination hyperbolas, located near one of the stations. This as well as the next two cases is plotted in Figure V.

#### Case 9.

This case utilized the same stations as case 8, and the same departure point, and great circle route, but had the destination short of the parallel hyperbolas. The destination and results were:

D    latitude ----- 63° 40' N  
     longitude ----- 45° 40' W

Great circle path length ----- 222 miles

Deviation from great circle -- 40 miles -- 18%

Excess Travel ----- 18 miles -- 8.2%

#### Case 10.

This case was plotted for the same stations as cases 8 and 9, utilizing the same departure point, and great circle route with the destination closer to the parallel hyperbolas than for Case 9. The destination and results were:

D    latitude ----- 63° 55' N  
     longitude ----- 41° 40' W

Great circle path length ----- 340 miles

Deviation from great circle ---- 132 miles -- 40%

Excess travel ----- 70 miles --- 21%



## APPENDIX B

In this appendix will be given the results of tests of the entire computer.

### Case 1.

For the first test of the computer, an idealized station configuration was chosen with stations in line and having equal separations. Hyperbolas for this test (in the plane only so as to leave out possible errors due to projection onto the earth) are drawn in figure 23, with the track obtained by plotting the points given in the data below:

<u>Point</u>	<u>TD<sub>XW</sub></u>	<u>Computed TD<sub>XY</sub></u>	<u>Computed distance to go</u>	<u>Actual distance to go</u>
D	375	1425	0	--
P <sub>0</sub>	1425	375	1200	---
P <sub>1</sub>	1350	789	860	890
P <sub>2</sub>	1200	1096	640	655
P <sub>3</sub>	900	1308	385	395
P <sub>4</sub>	600	1387	178	182
P <sub>5</sub>	375	1426	0.7	0

The maximum deviation from the straight line track in the plane was 10 miles.



Case 2.

For this trial, a course was run between points on the meridian  $45^{\circ}$  W, with the following results:

<u>Point</u>	<u>TD<sub>XW</sub></u>	<u>Computed TD<sub>XY</sub></u>	<u>Miles off track</u>
D	1-L-4-6705	1-L-3-1660	
P <sub>0</sub>	2752	3720	
P <sub>1</sub>	3000	3681	0 west of track
P <sub>2</sub>	3400	3329	7
P <sub>3</sub>	4200	2605	9
P <sub>4</sub>	5000	2147.5	5
P <sub>5</sub>	6000	1800	5
P <sub>6</sub>	6705	1660	0

Case 3. Track along meridian  $35^{\circ}$  W.

<u>Point</u>	<u>TD<sub>XW</sub></u>	<u>Computed TD<sub>XY</sub></u>	<u>Miles off track</u>
D	1-L-3-1900	1-L-4-7744	
P <sub>0</sub>	3300	4440	0
P <sub>1</sub>	3000	5010.5	5 west of track
P <sub>2</sub>	2700	5613	10
P <sub>3</sub>	2400	6305.5	11
P <sub>4</sub>	2100	7139.5	11
P <sub>5</sub>	2000	7438.5	7
P <sub>6</sub>	1950	---	5
P <sub>7</sub>	1900	7744	0





Case 4.

This case was run to test the stability of approach to destination, and the same problem was set up as for case 3, but only the last 15 miles of the problem was worked.

<u>TD<sub>XY</sub></u>	<u>TD<sub>XW</sub></u> <u>Computed</u>	<u>Computed Dist. to go</u>
1-L-3-1920	1-L-4-7677	14.2
1-L-3-1910	7709	7.6
1905	7723.5	4.2
1902.5	7728	3.3
1901	7733.5	2.0
1900	7737	1.3
1899	--	0.3
1898	7744.5	0.18
1896	--	0.51
1890	7770	6.0
1880	7797	12.5
1850	7879	32.0

From the data plotted it can be seen that the destination vector shifted slightly after setting it at the start of the problem, since the closest approach as indicated by distance to go did not occur at the destination coordinates. After reaching the destination, the plane will follow a straight course along the same great circle away from the destination, with no violent transient at the destination.



Case 5.

The same problem as for case 3 was worked, with a 350 microsecond error purposely introduced in station base  $B_W$ .  $B_W$  equal to 1500 microseconds. 820 mile path.

<u>Point</u>	<u>TD<sub>XY</sub></u>	<u>Computed TD<sub>XW</sub></u>	<u>Miles off track</u>
D	1-L-3-1900	1-L-4-7744	
P <sub>0</sub>	3300	4400	
P <sub>1</sub>	3000	5000	10
P <sub>2</sub>	2700	5586	17
P <sub>3</sub>	2400	6268	22
P <sub>4</sub>	2100	7097	23
P <sub>5</sub>	2000	7415	17
P <sub>6</sub>	1940	7611	10
P <sub>7</sub>	1920	7677	6
P <sub>8</sub>	1900	7744	0

Case 6.

The same problem as 3, 4, and 5, but with  $B_W$  base line set with the opposite error.  $B_W$  equal to 1300 microseconds.

<u>Point</u>	<u>TD<sub>XY</sub></u>	<u>Computed TD<sub>XW</sub></u>	<u>Miles off track</u>
P <sub>1</sub>	1-L-3-3000	1-L-4-5010	2 West of track
P <sub>2</sub>	2700	5617	6
P <sub>3</sub>	2400	6332	2
P <sub>4</sub>	2100	7157	1
P <sub>5</sub>	2000	7452	2
P <sub>6</sub>	1940	7627	3
P <sub>7</sub>	1920	7682	3
P <sub>8</sub>	1900	7774.5	0



## BIBLIOGRAPHY

1. Frank, R. L. "Description of Loran Automatic Navigator" P.N. 5140801 - Feb. 6, 1950 - Sperry Gyroscope Company, Great Neck, New York.
2. Frantz, W. P. Laboratory Notebook No. 1636, Pg. 91-100. Sperry Gyroscope Company, Great Neck, New York.
3. Palmer, W. "Project Report Study of Loran Digital Computer" 37 pages - Report No. 5223-1149 for Sperry Gyroscope Company, Great Neck, New York.
4. Pierce, "Loran" Massachusetts Institute of Technology - Radiation Laboratory - Series No. 4 - New York, McGraw-Hill.
5. Streeter, Edward C. Jr. U.S. Patent No. 2,472,129, June 17, 1949, "Radio Navigation System".





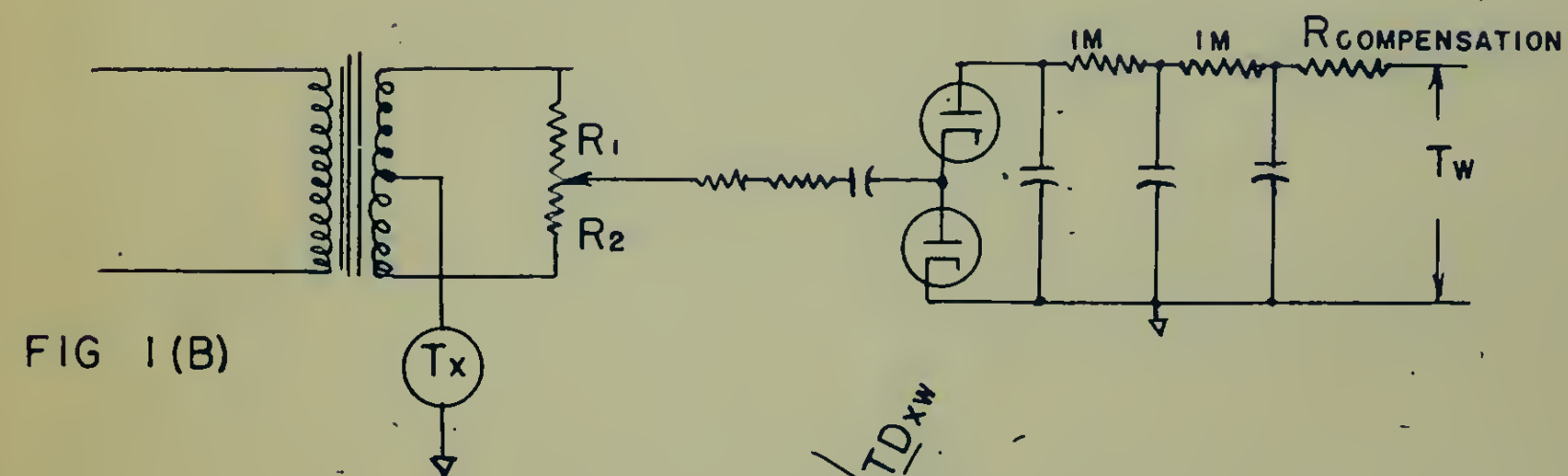
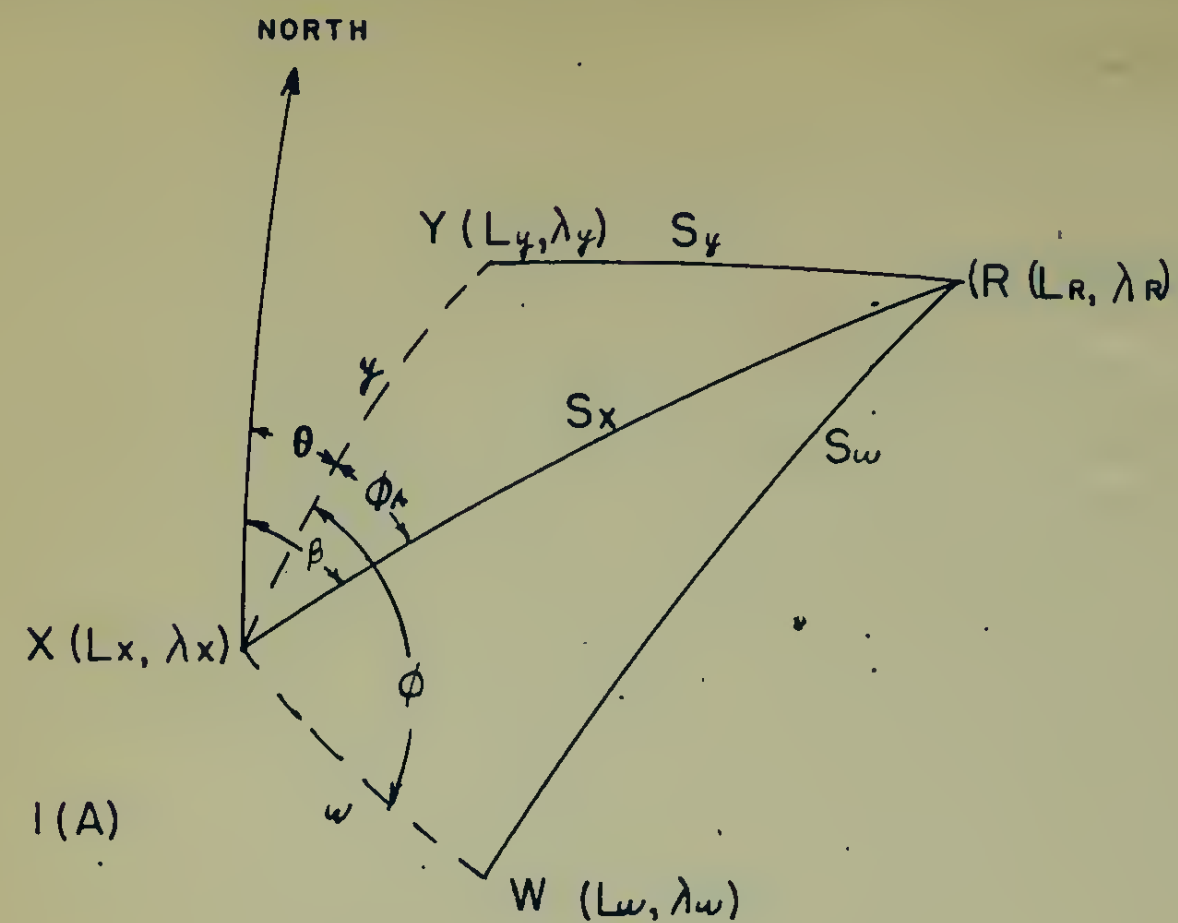
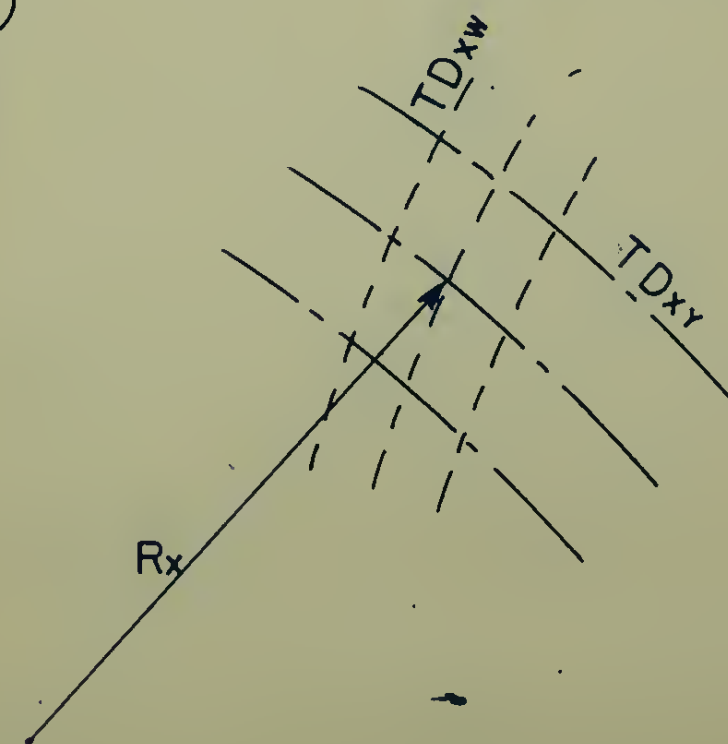
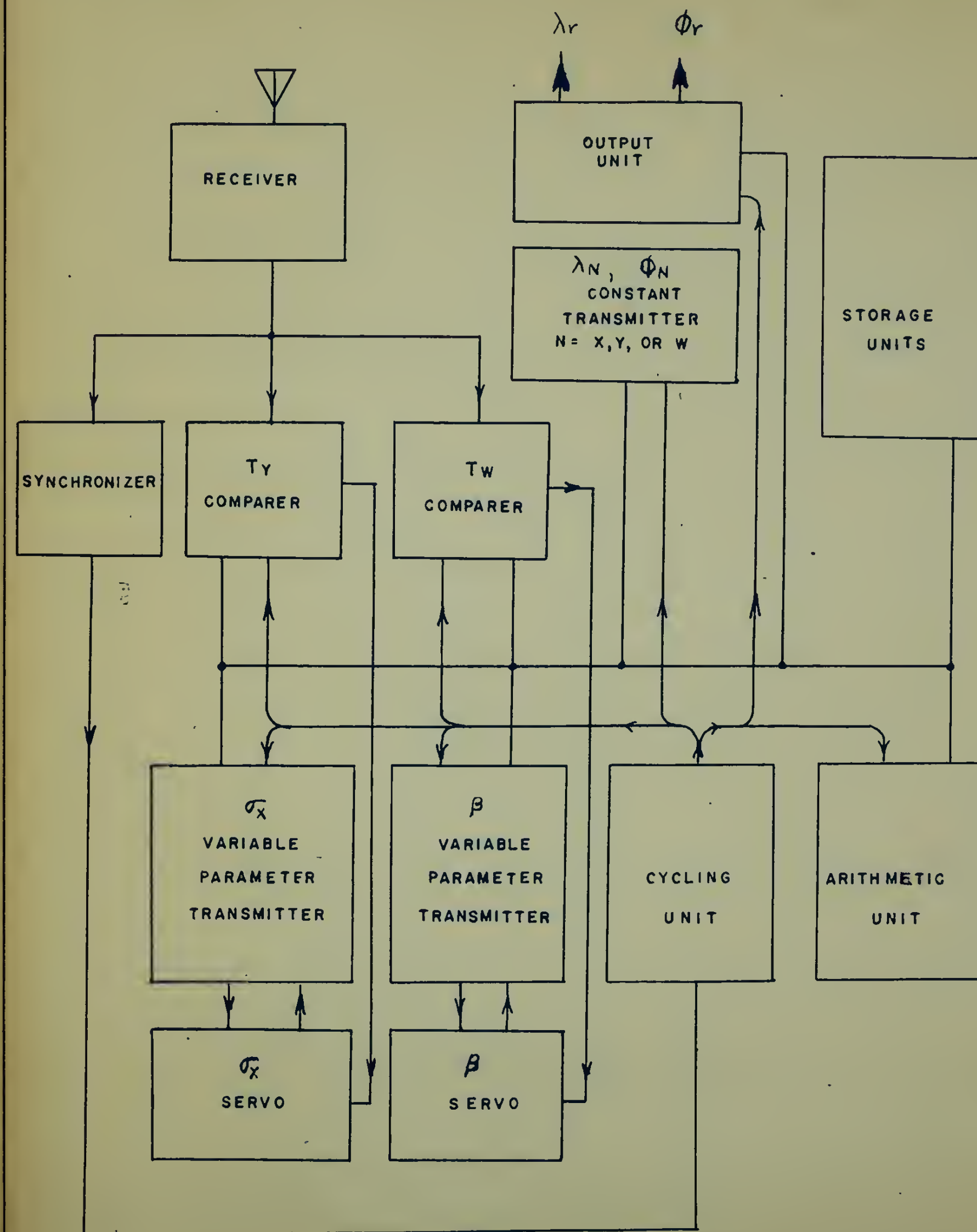


FIG 1(C)

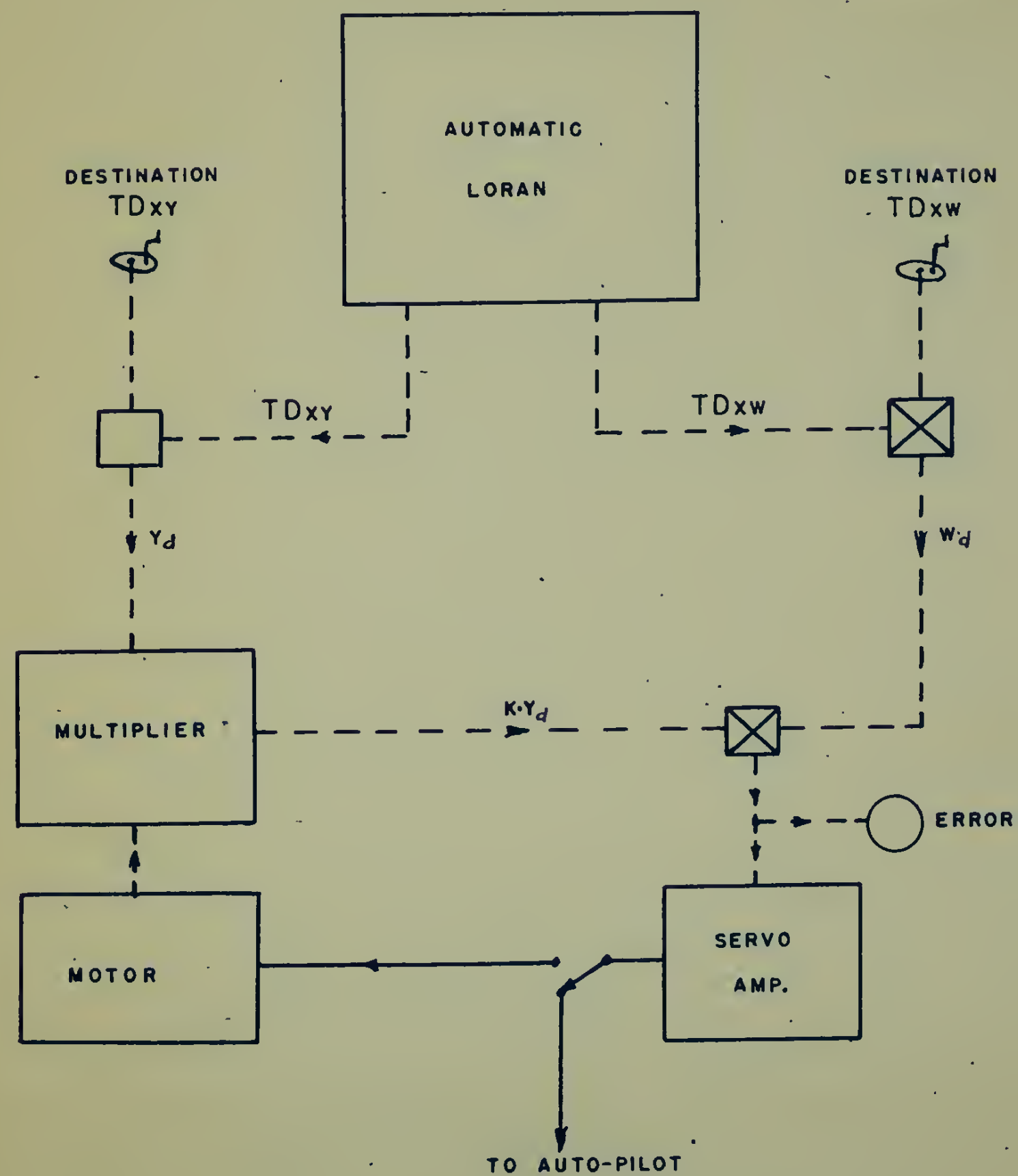






DIGITAL HYPERBOLIC COMPUTER BLOCK DIAGRAM





LORHUMB COMPUTER

SPERRY GYROSCOPE CO.

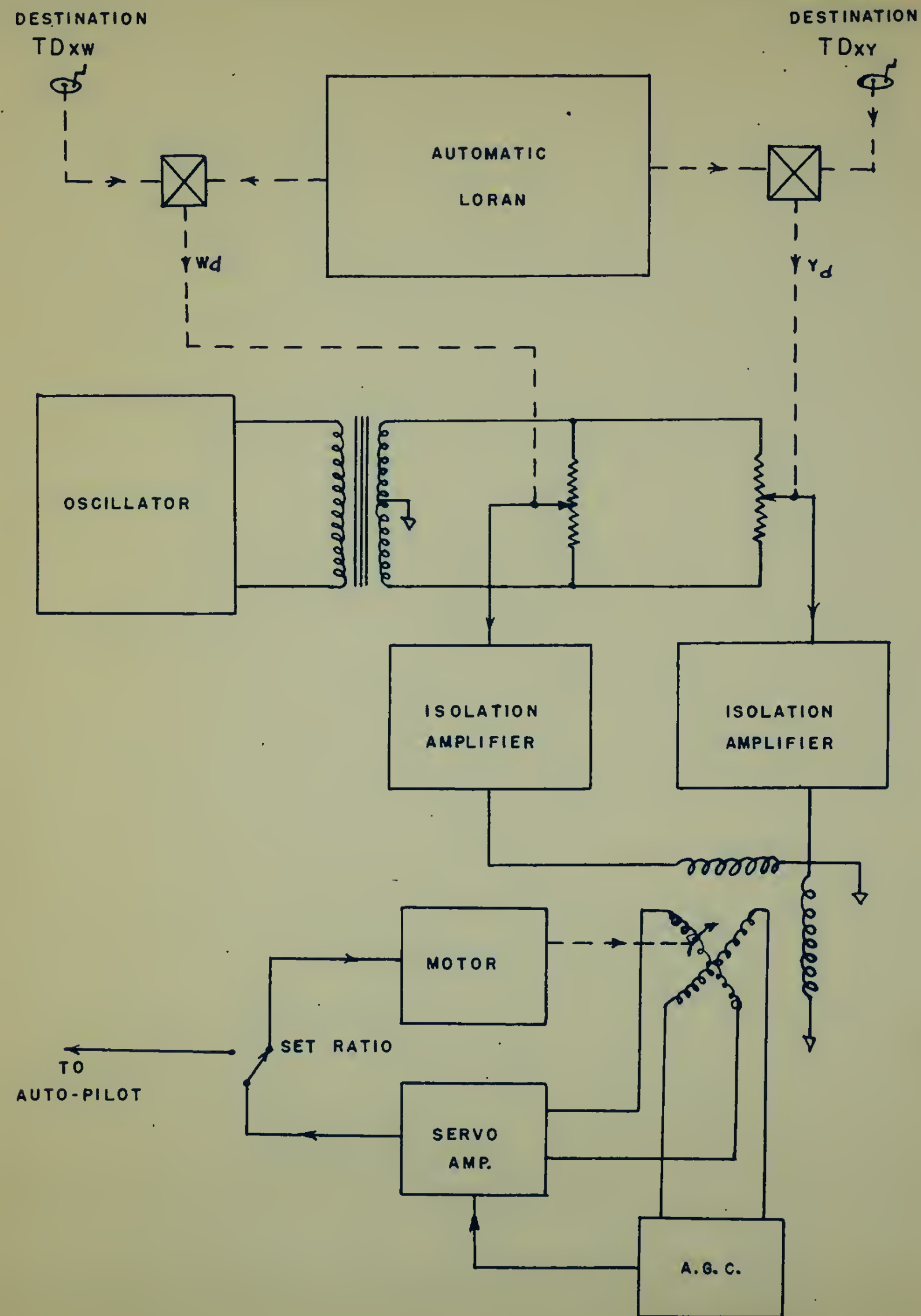
DATE 2/27/50

ENG. *W. M. T.*

SK. No. 3







ELECTRONIC LORHUMB COMPUTER

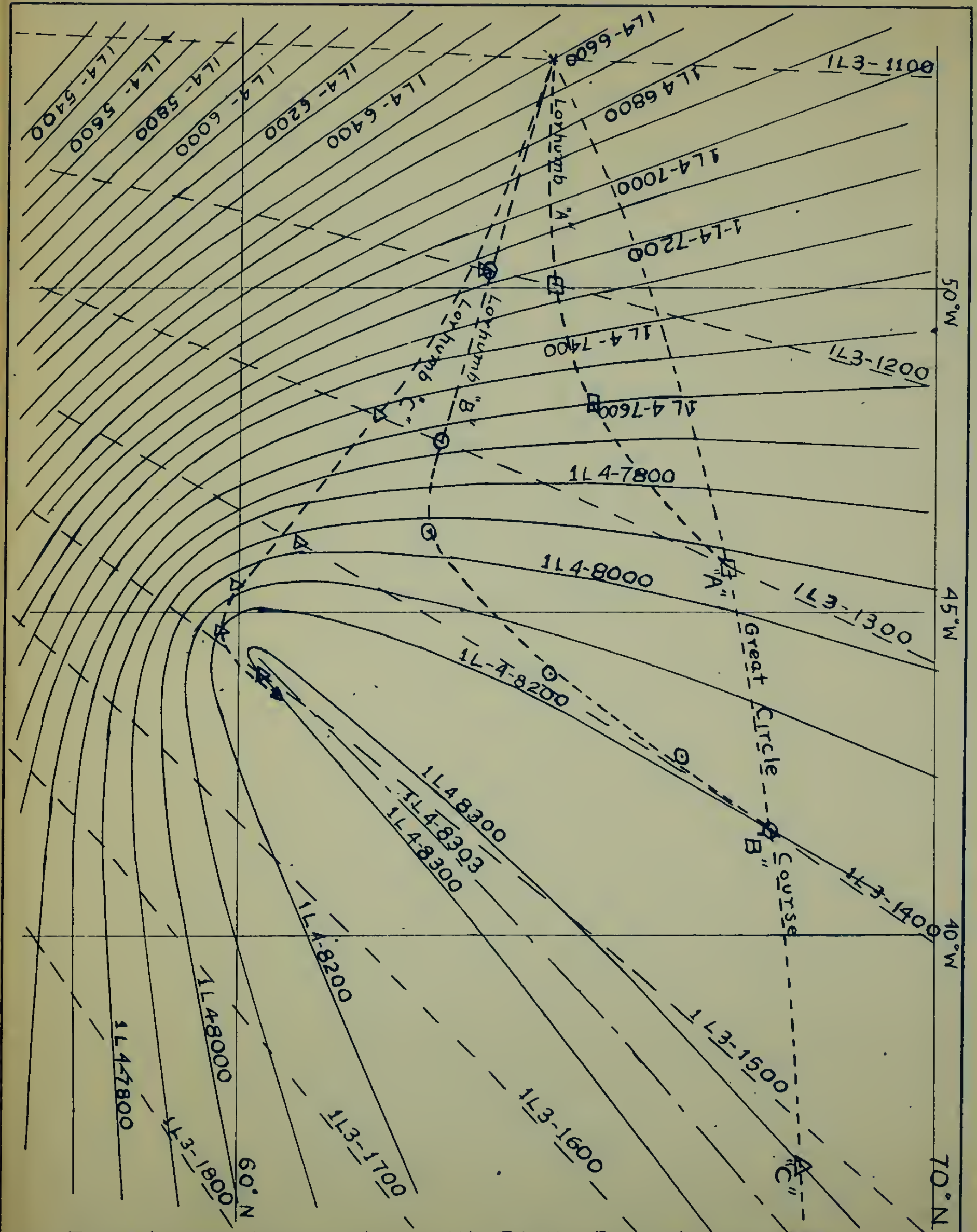
SPERRY GYROSCOPE CO.

DATE 2/27/50

ENG. *WIM T*

SK. No. 4





Departure of Lorchumb Lines From Great Circle.

SPERRY GYROSCOPE CO.

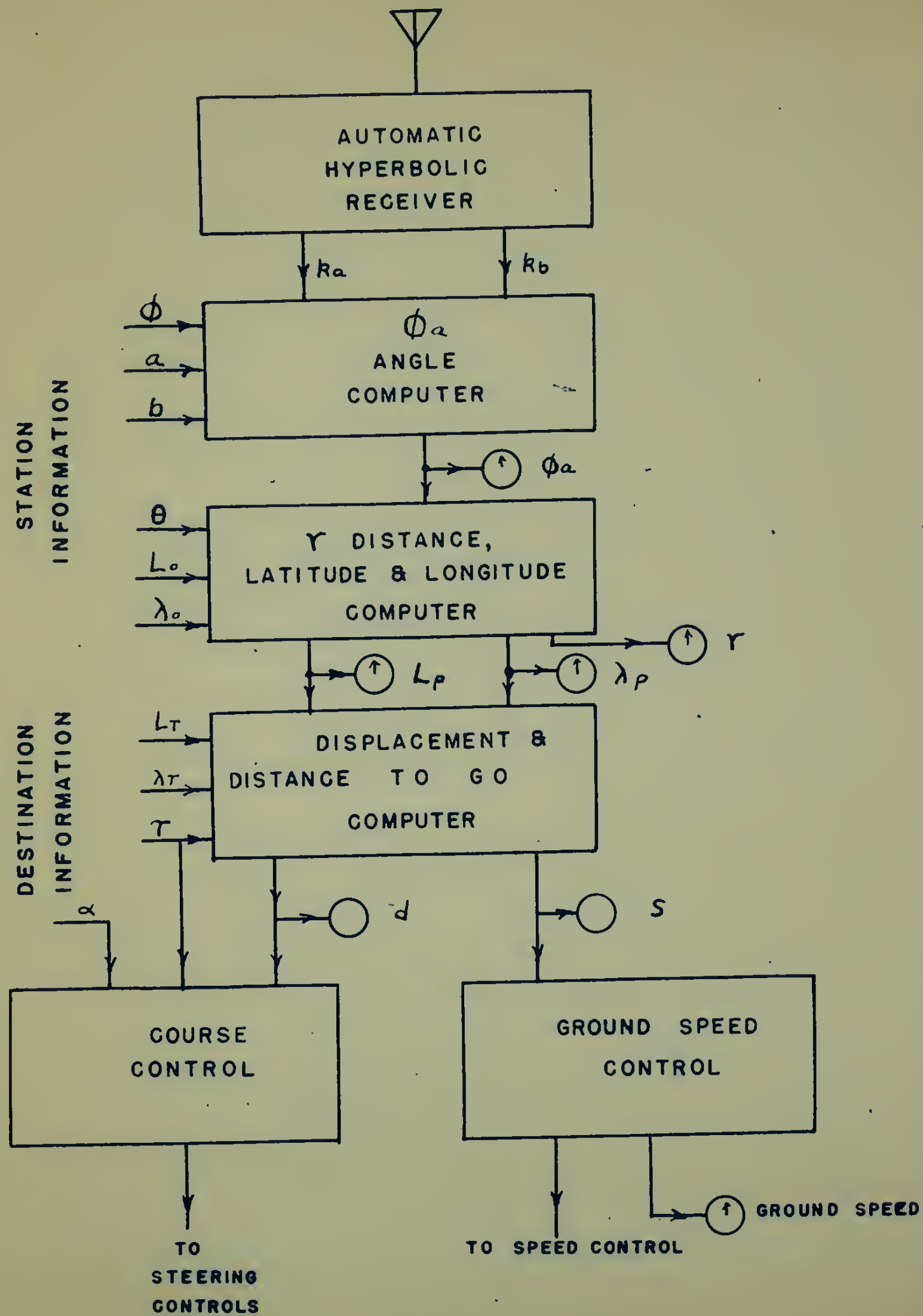
DATE 2/27/50

ENG. W. M. G.

SK. No. 5







STREETER HYPERBOLIC COMPUTER

SPERRY GYROSCOPE CO.

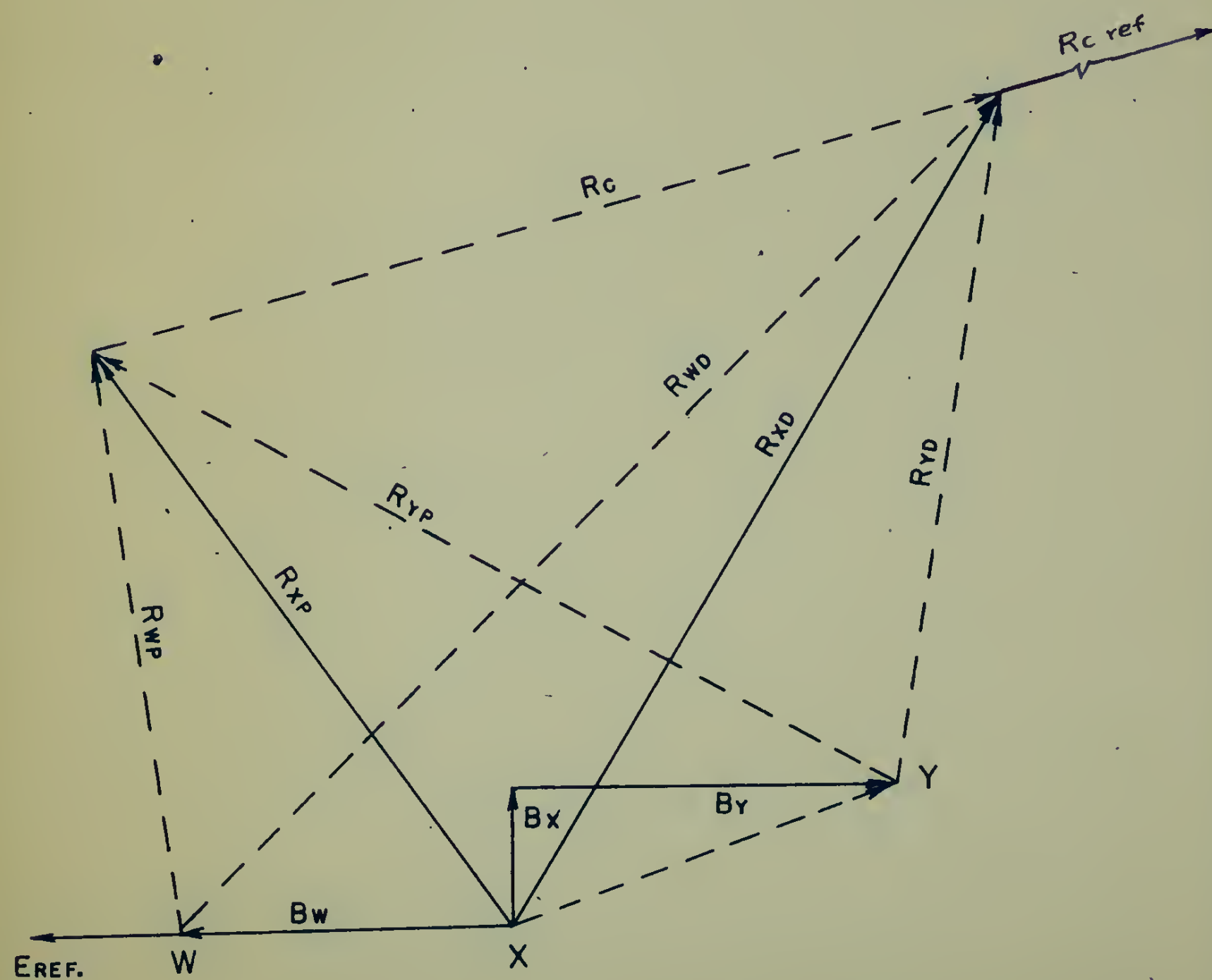
DATE 2/27/50

ENG. W. M. T.

SK. No. 6







LORAN COMPUTER VECTOR DIAGRAM

SPERRY GYROSCOPE CO.

DATE 2/27/50

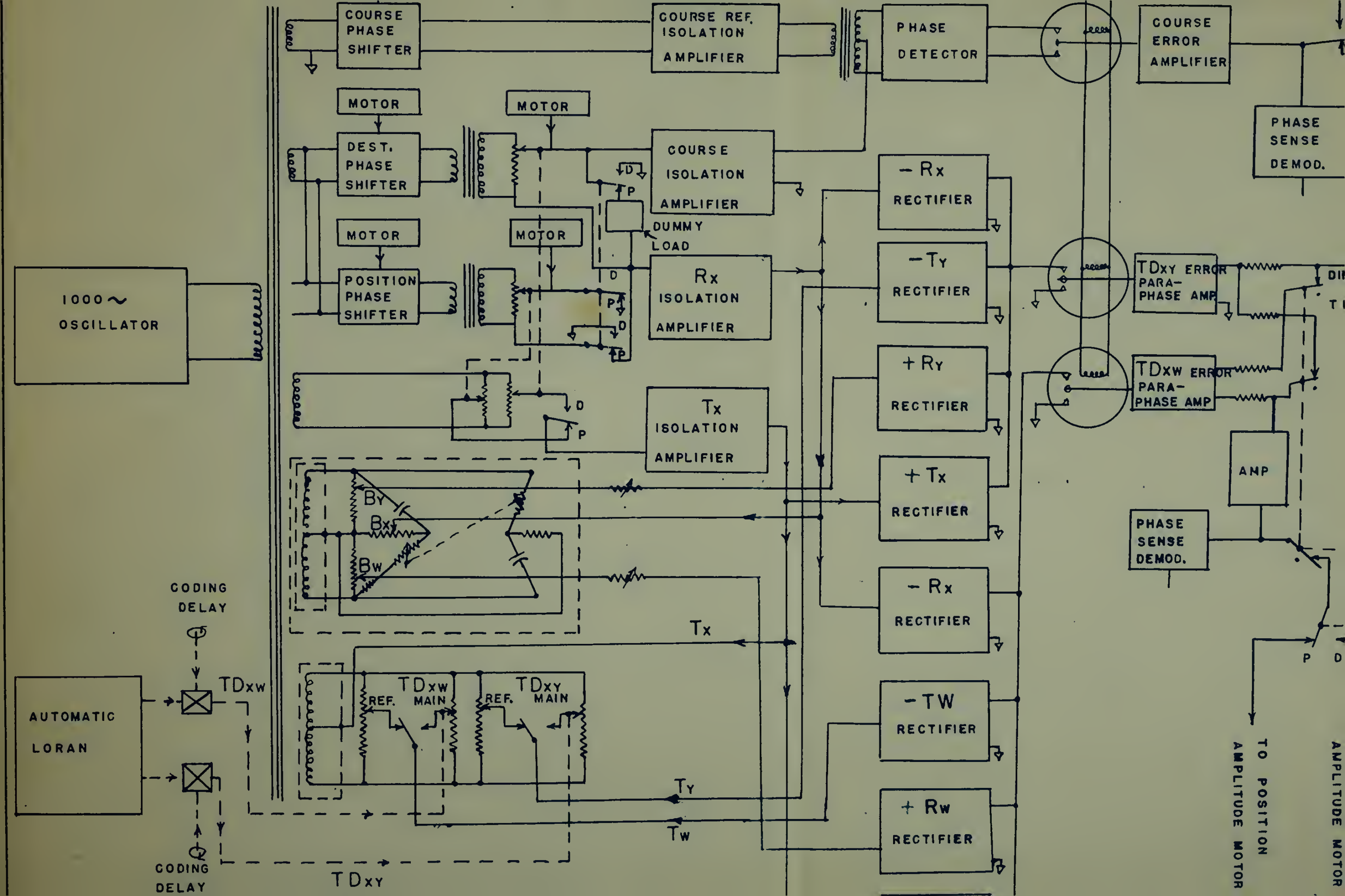
ENG. *Wm J*

SK. No. 7



MERCATOR AND HYPERBOLIC PROJECTIONS OF NEWFOUNDLAND			
SPERRY GYROSCOPE CO.	DATE. 2/27/50	ENG. <i>Wmmt</i>	SK. No. 8



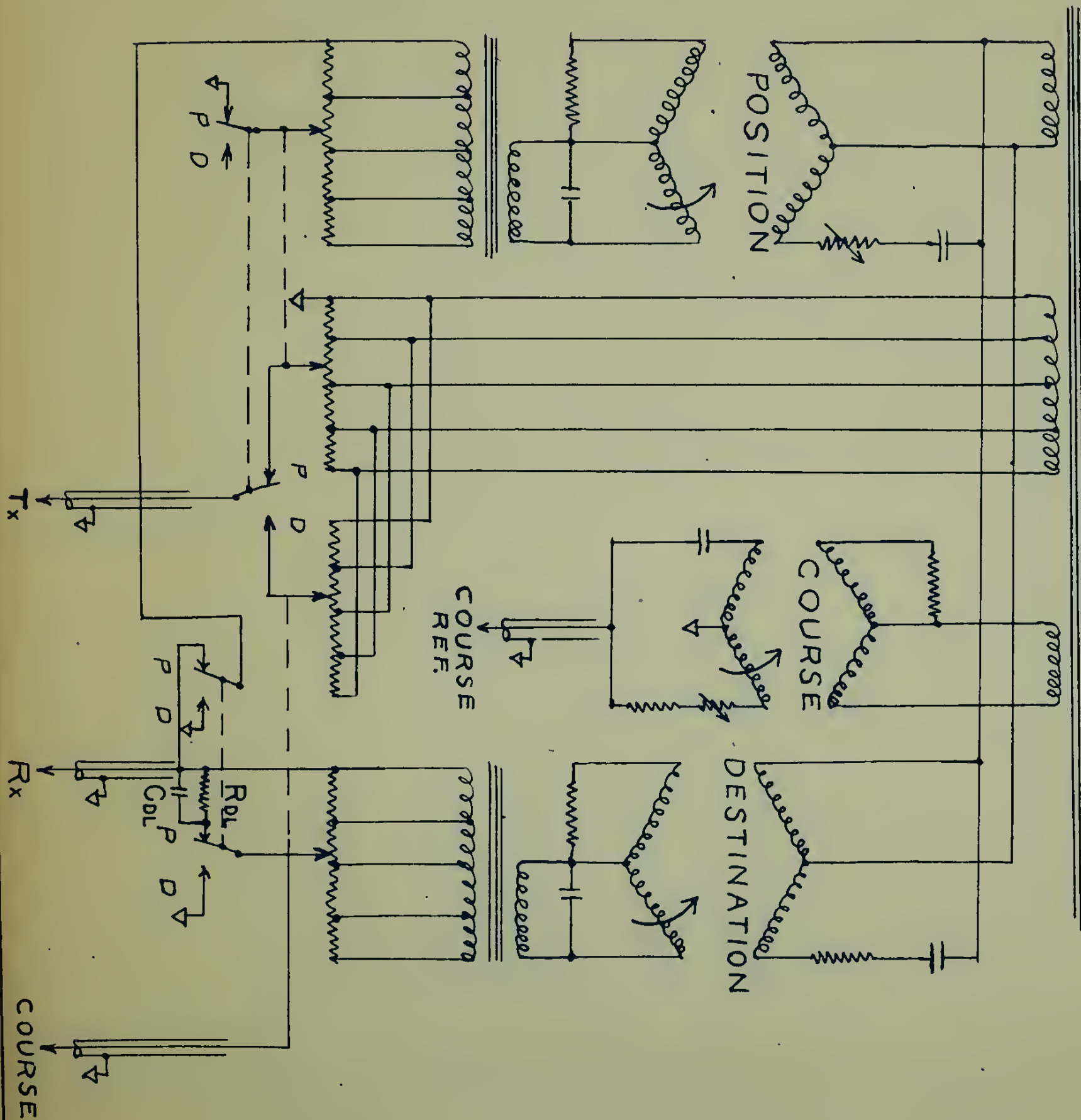












# PHASE SHIFTER CHASSIS

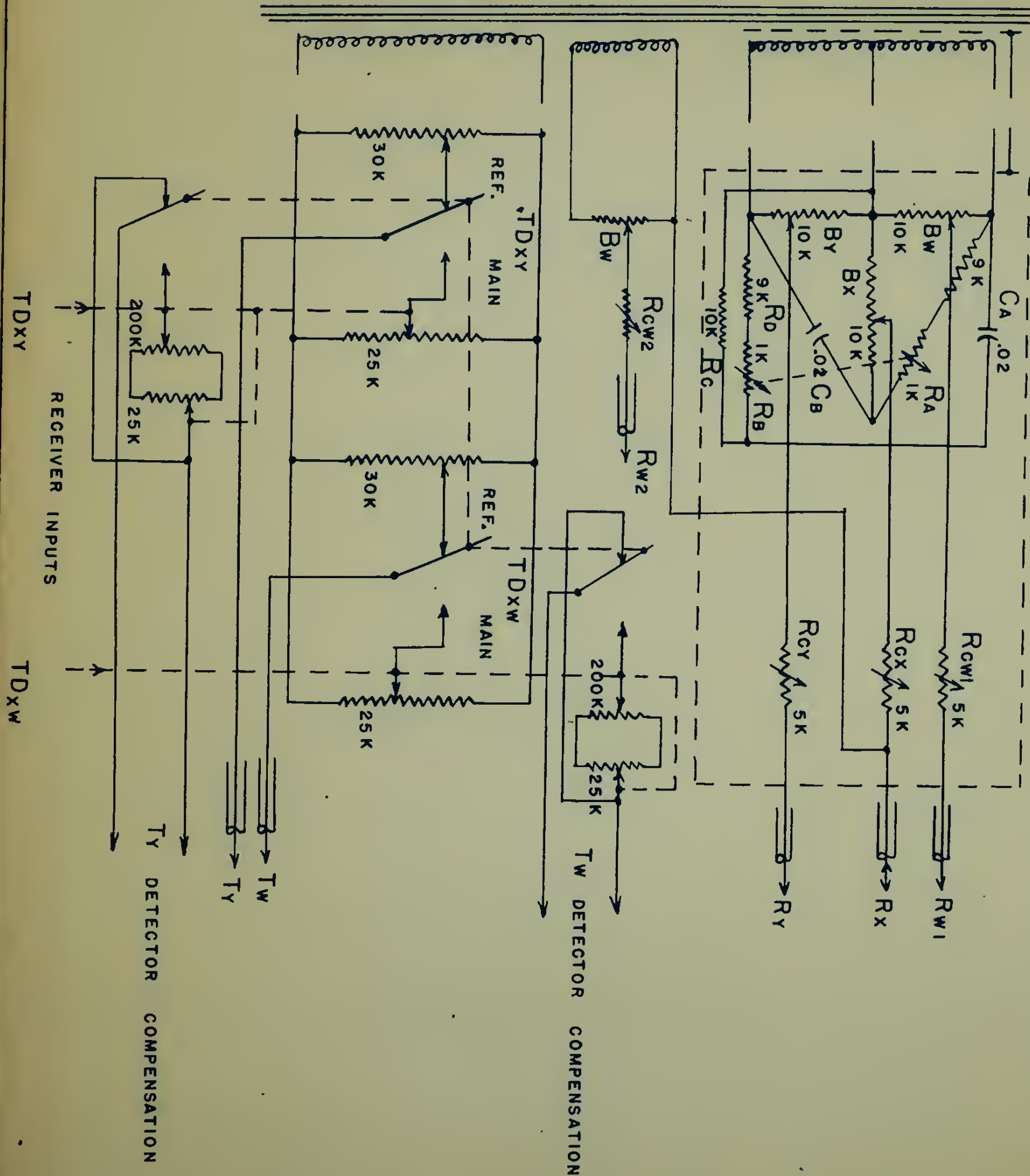
SPERRY GYROSCOPE CO.

DATE 2/27/50

ENG. W. M. G.

SK. No. 11





STATION	BASLINE	&	TIME	DIFFERENCE	CHASSIS
1	100		100		100
2	100		100		100
3	100		100		100
4	100		100		100
5	100		100		100
6	100		100		100
7	100		100		100
8	100		100		100
9	100		100		100
10	100		100		100
11	100		100		100
12	100		100		100
13	100		100		100
14	100		100		100
15	100		100		100
16	100		100		100
17	100		100		100
18	100		100		100
19	100		100		100
20	100		100		100
21	100		100		100
22	100		100		100
23	100		100		100
24	100		100		100
25	100		100		100
26	100		100		100
27	100		100		100
28	100		100		100
29	100		100		100
30	100		100		100
31	100		100		100
32	100		100		100
33	100		100		100
34	100		100		100
35	100		100		100
36	100		100		100
37	100		100		100
38	100		100		100
39	100		100		100
40	100		100		100
41	100		100		100
42	100		100		100
43	100		100		100
44	100		100		100
45	100		100		100
46	100		100		100
47	100		100		100
48	100		100		100
49	100		100		100
50	100		100		100
51	100		100		100
52	100		100		100
53	100		100		100
54	100		100		100
55	100		100		100
56	100		100		100
57	100		100		100
58	100		100		100
59	100		100		100
60	100		100		100
61	100		100		100
62	100		100		100
63	100		100		100
64	100		100		100
65	100		100		100
66	100		100		100
67	100		100		100
68	100		100		100
69	100		100		100
70	100		100		100
71	100		100		100
72	100		100		100
73	100		100		100
74	100		100		100
75	100		100		100
76	100		100		100
77	100		100		100
78	100		100</		

SPERRY GYROSCOPE CO.

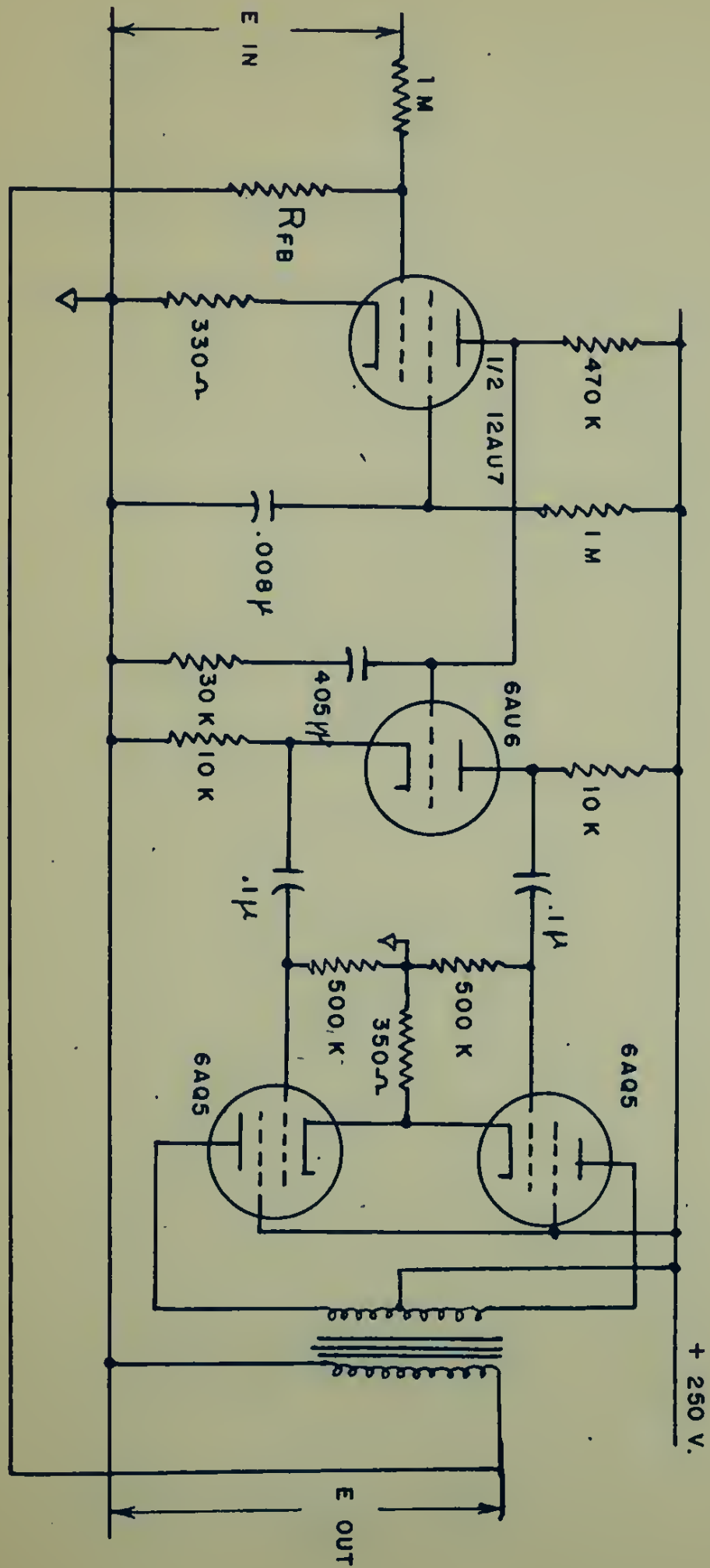
DATE. 2/27/50

ENG. *WMT*

SK. No. 12







## ISOLATION AMPLIFIER

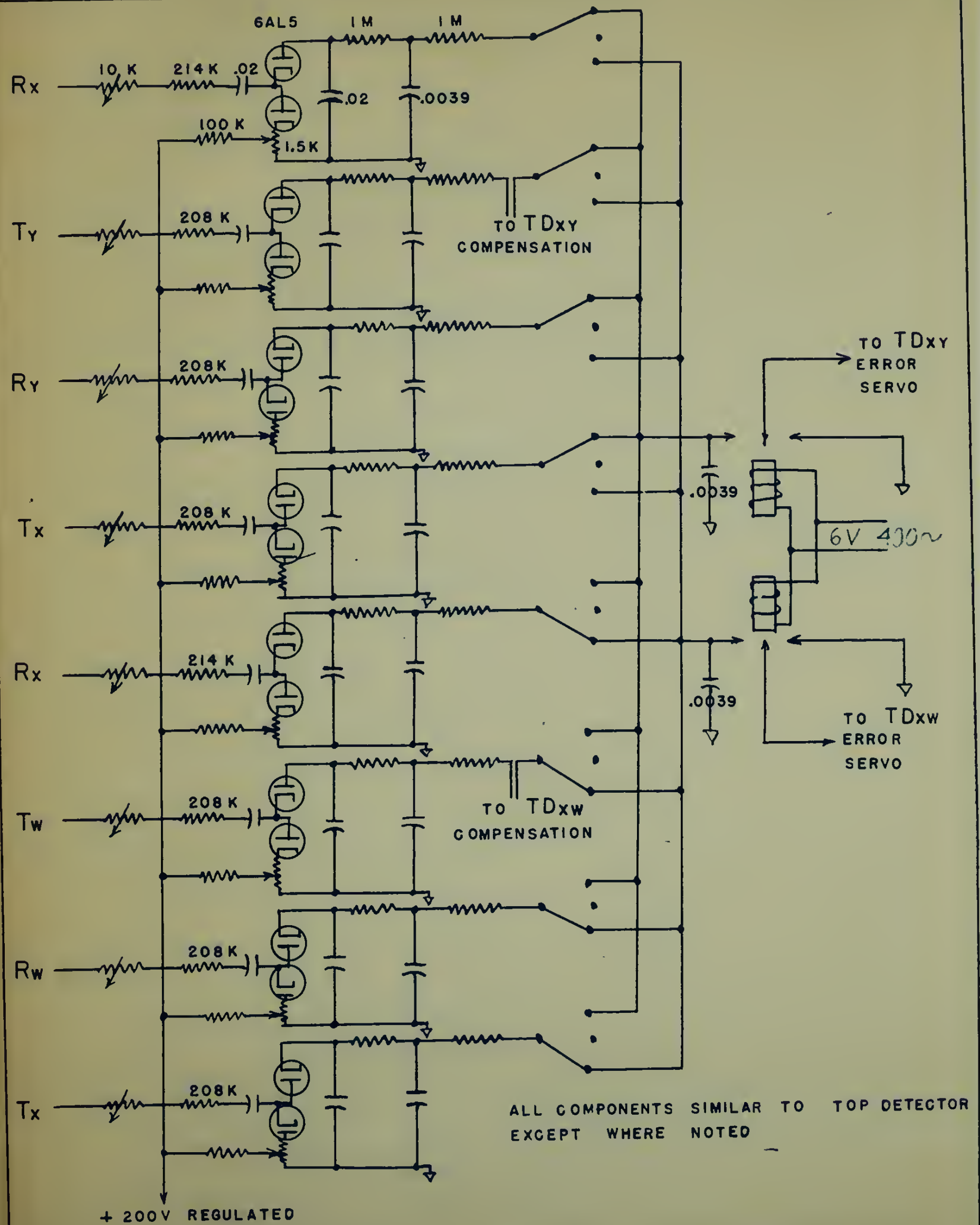
SPERRY GYROSCOPE CO.

DATE 2/27/50

ENG. *W. M. T.*

SK. No. 13





DETECTOR SUB-CHASSIS

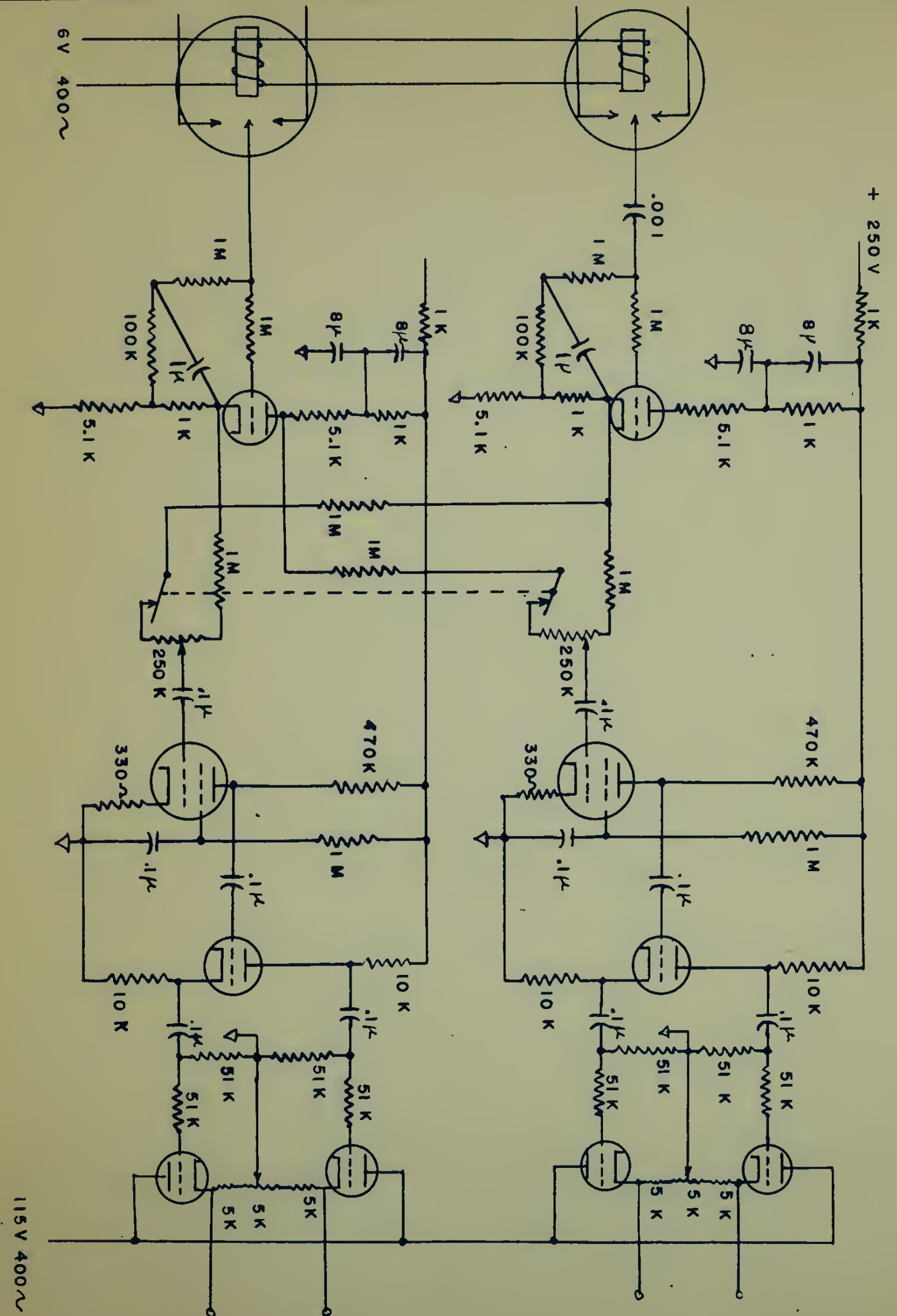
SPERRY GYROSCOPE CO.

DATE 2/27/50

ENG. *W M T*

SK. No. 14





## SERVO AMPLIFIER

SPERRY GYROSCOPE CO.

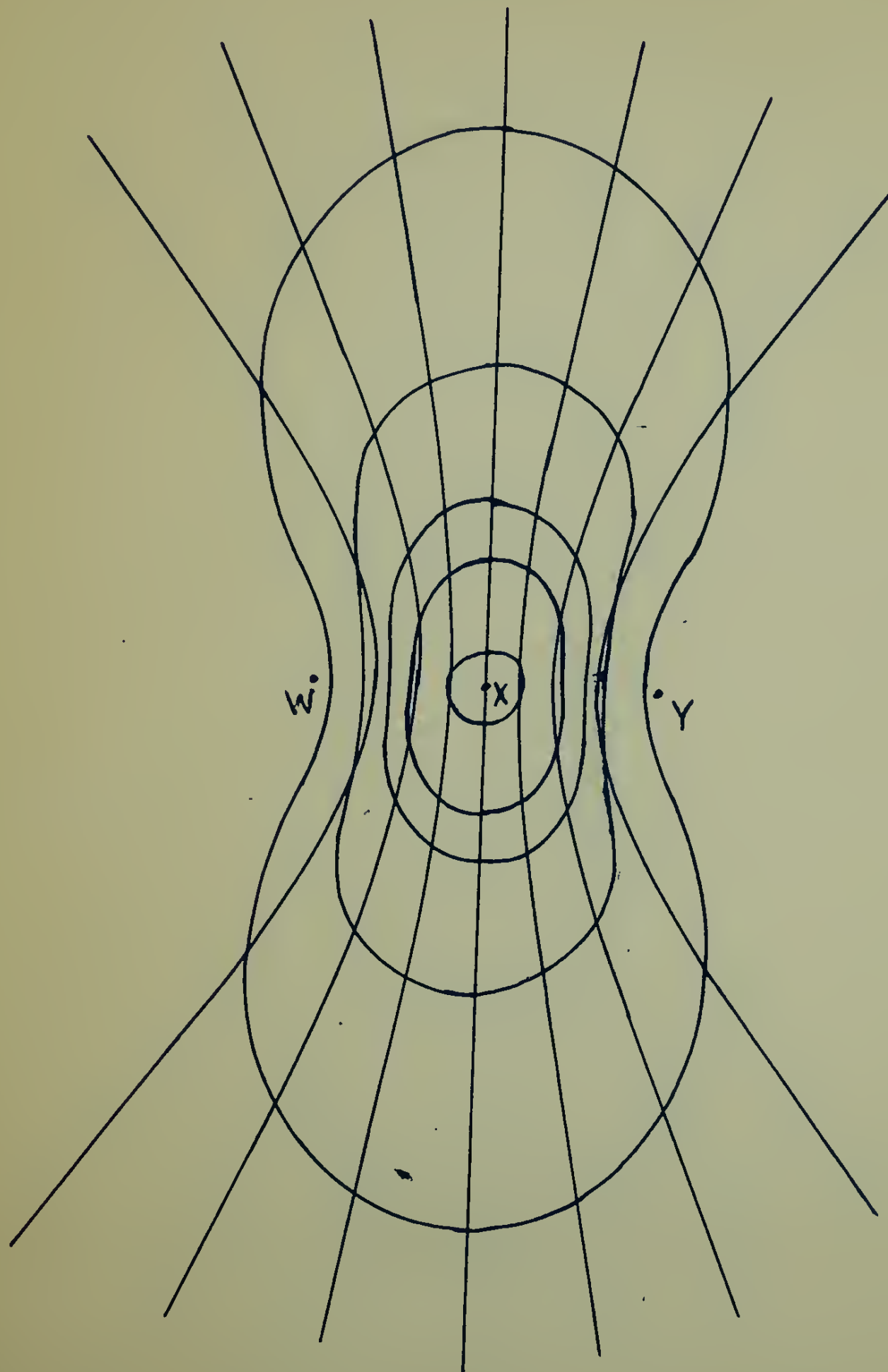
DATE. 2/27/50

ENG. *W M J*

SK. No. 15





LOCUS OF SUM & DIFFERENCE OF TIME DIFFERENCES  $TD_{xw}$  &  $TD_{xy}$ 

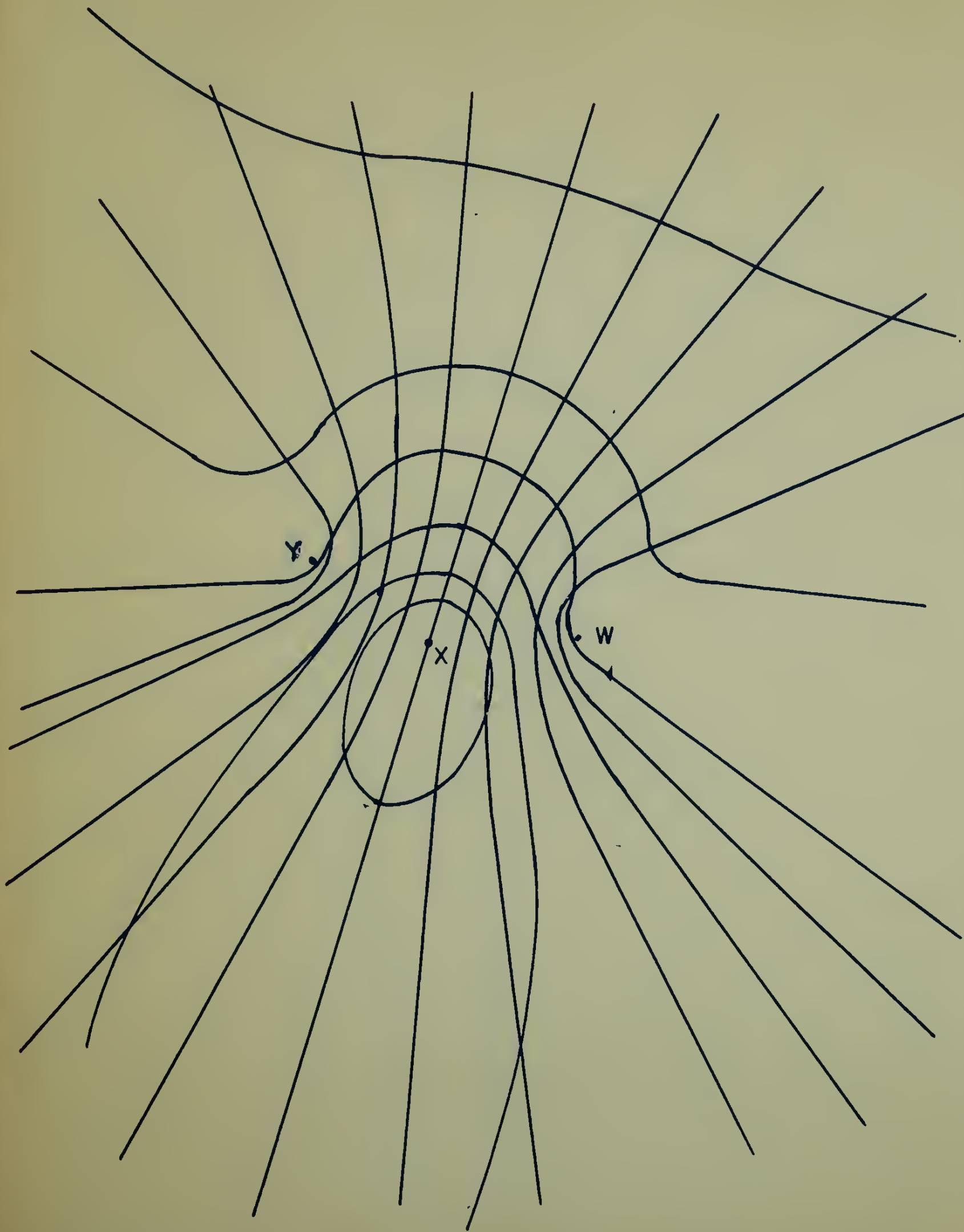
SPERRY GYROSCOPE CO.

DATE 2/27/50

ENG. *N.M.T.*

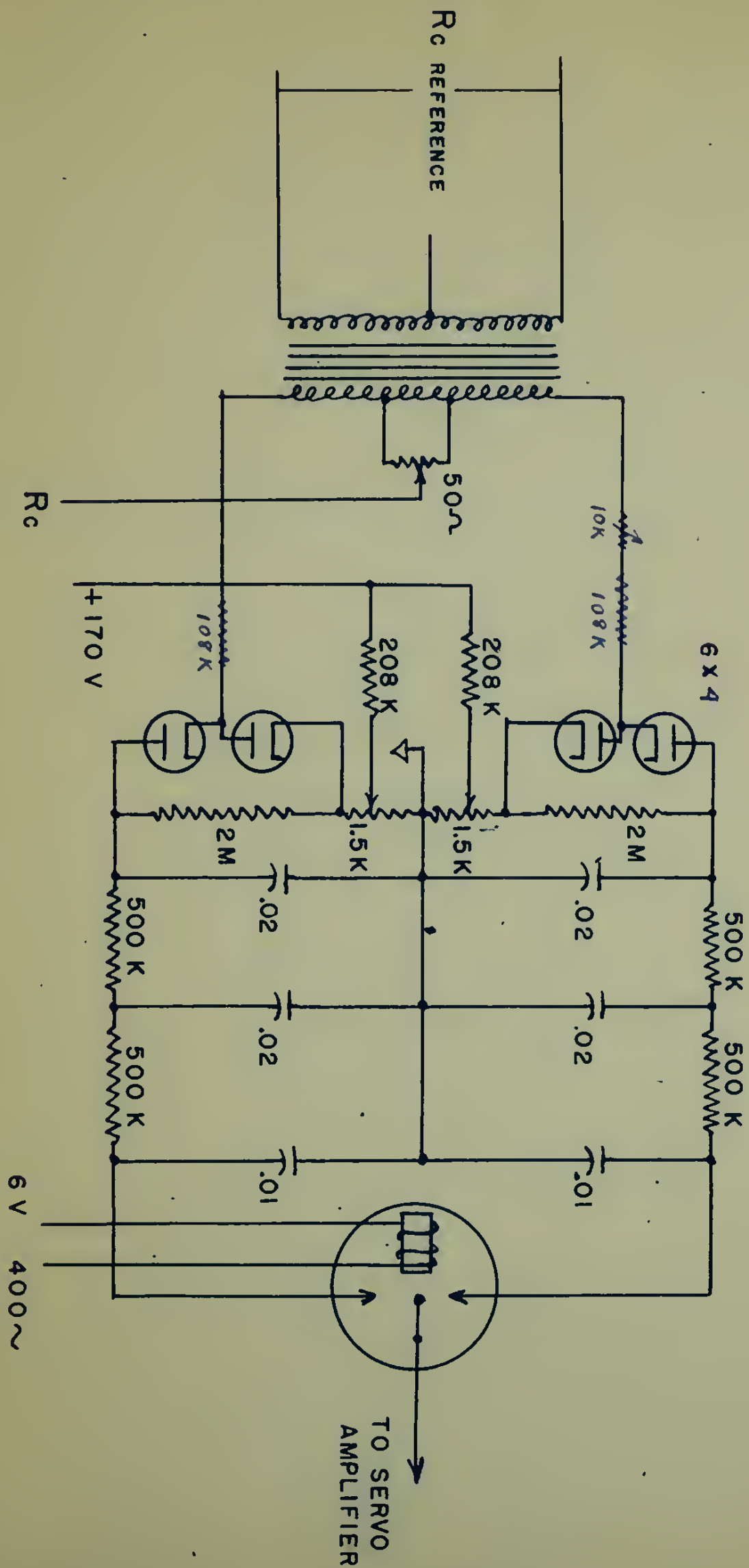
SK. No. 16





LOCUS OF SUM & DIFFERENCE OF TIME DIFFERENCES	TD <sub>xy</sub> & TD <sub>xw</sub>
SPERRY GYROSCOPE CO.	DATE. 2/27/50      ENG. <i>wmt</i> SK. No. 17

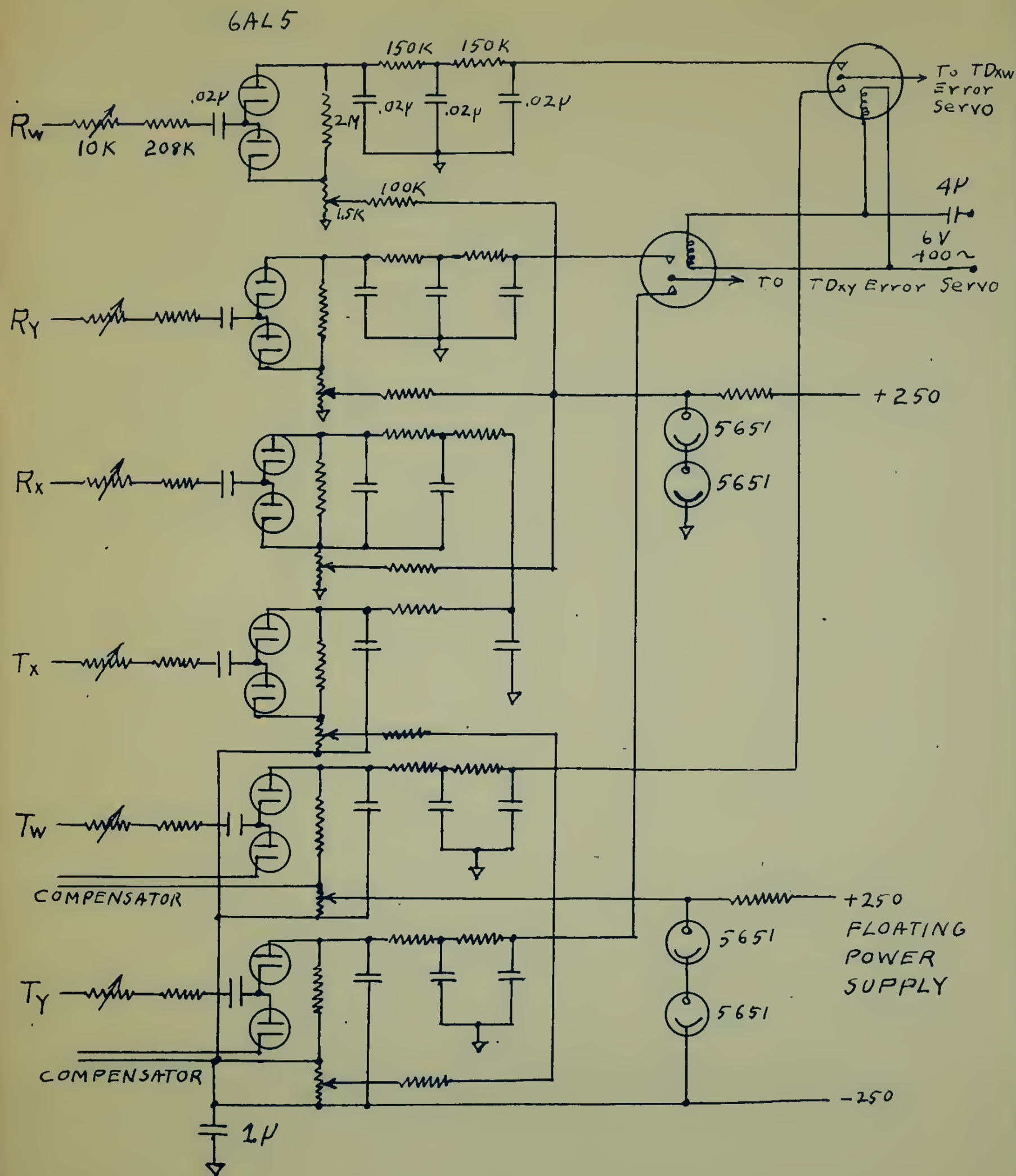




## PHASE DETECTOR







DETECTOR SUB CHASSIS (FIRST)

SPERRY GYROSCOPE CO.

DATE 2/27/50

ENG. W.M.T.

SK. No. 19



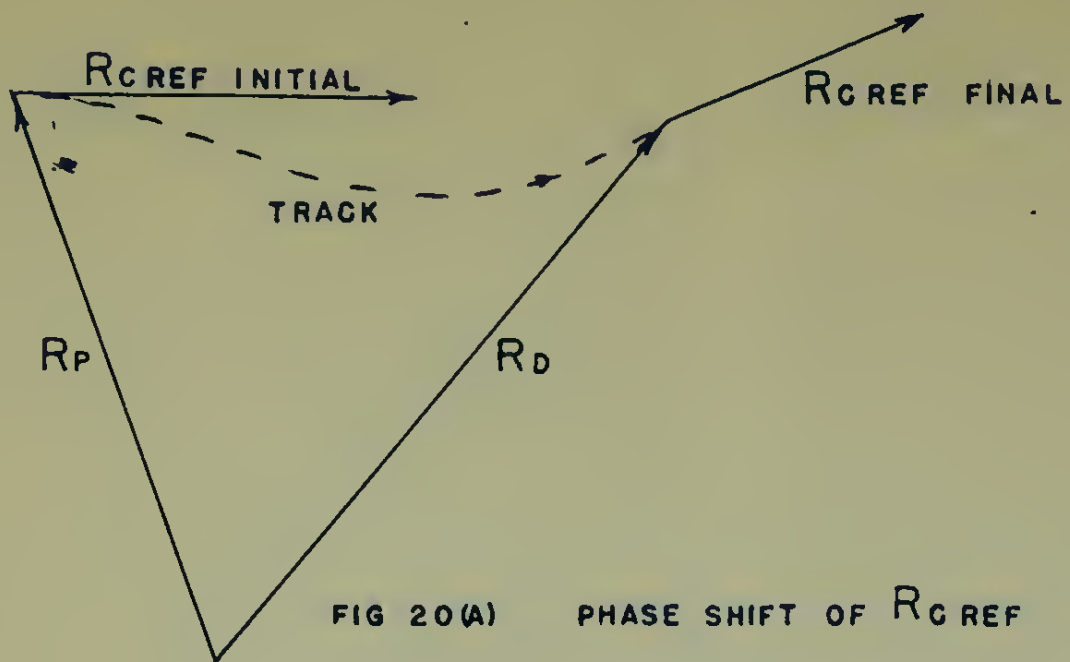


FIG 20(A) PHASE SHIFT OF  $R_C$  REF

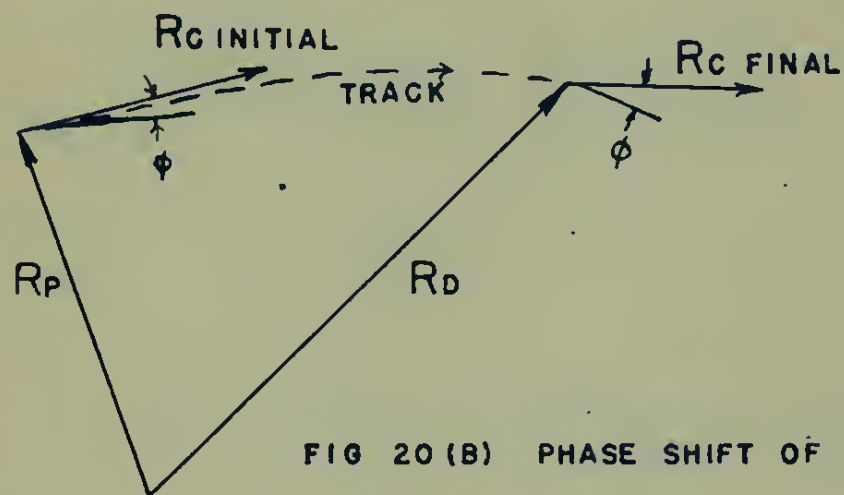


FIG 20(B) PHASE SHIFT OF  $R_C$

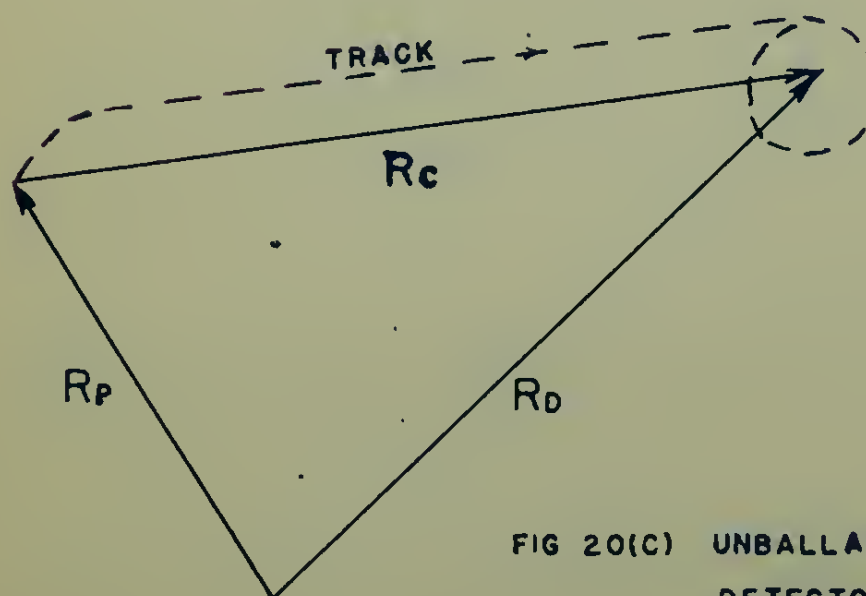
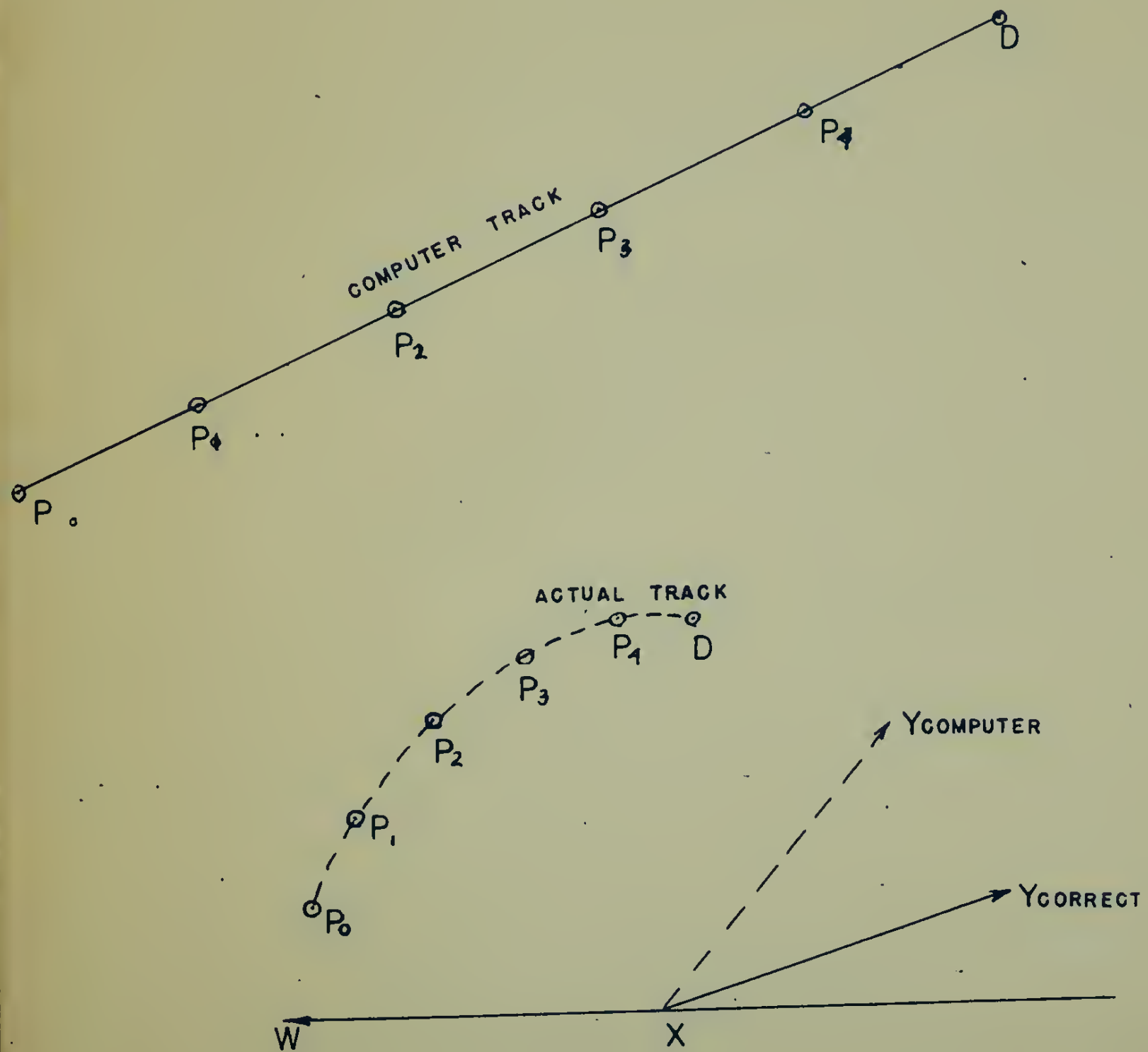


FIG 20(C) UNBALLANCE OF PHASE  
DETECTOR OR SERVO

TRACKS WITH SYSTEM ERRORS





30° ERROR IN XY BASELINE

SPERRY GYROSCOPE CO.

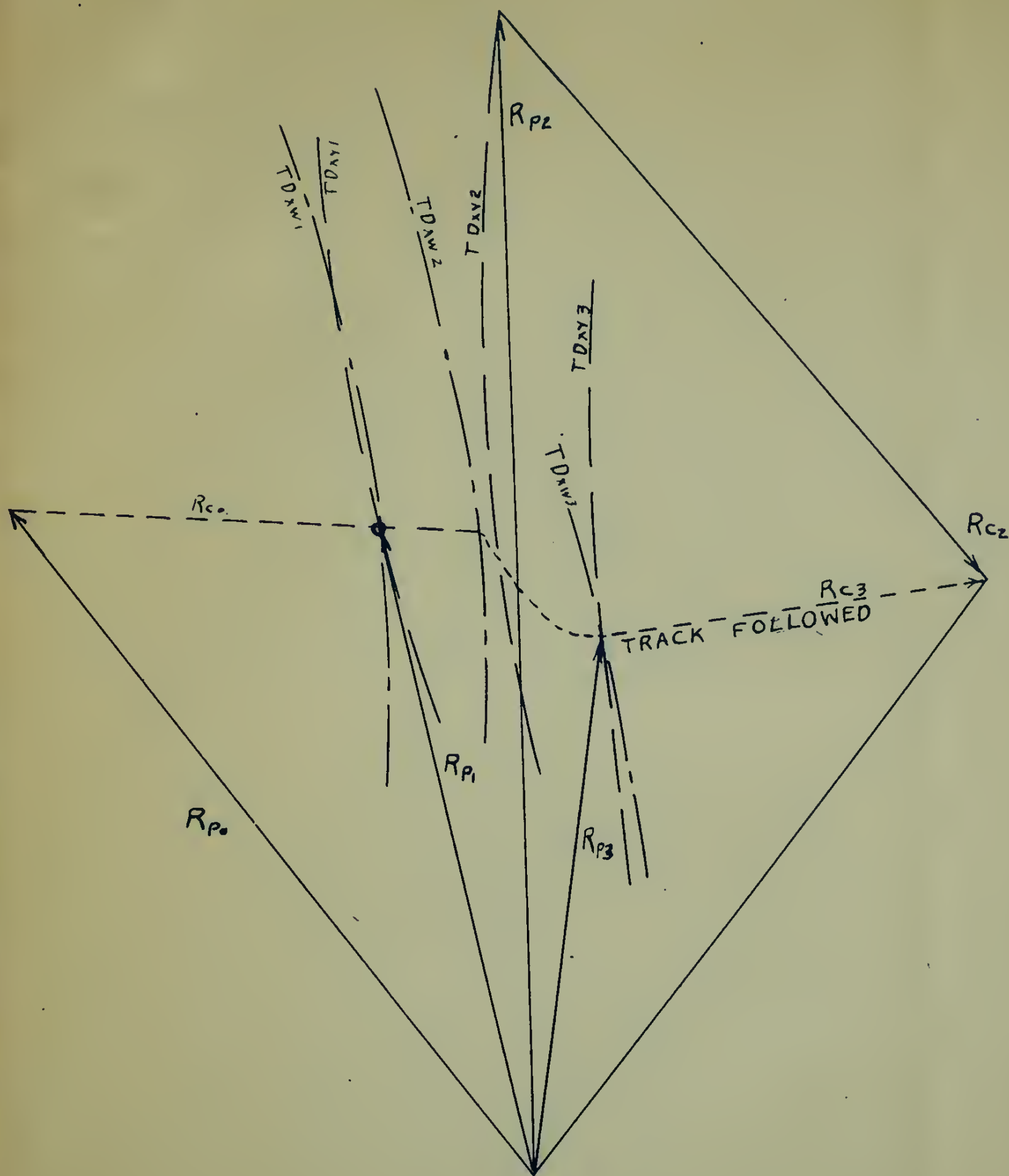
DATE 2/27/50

ENG. WMT

SK. No. 21







# PATH DUE TO NON INTERSECTION OF PLANE HYPERBOLAS

**SPERRY GYROSCOPE CO.**

DATE 2/27/50

ENG. *WMT*

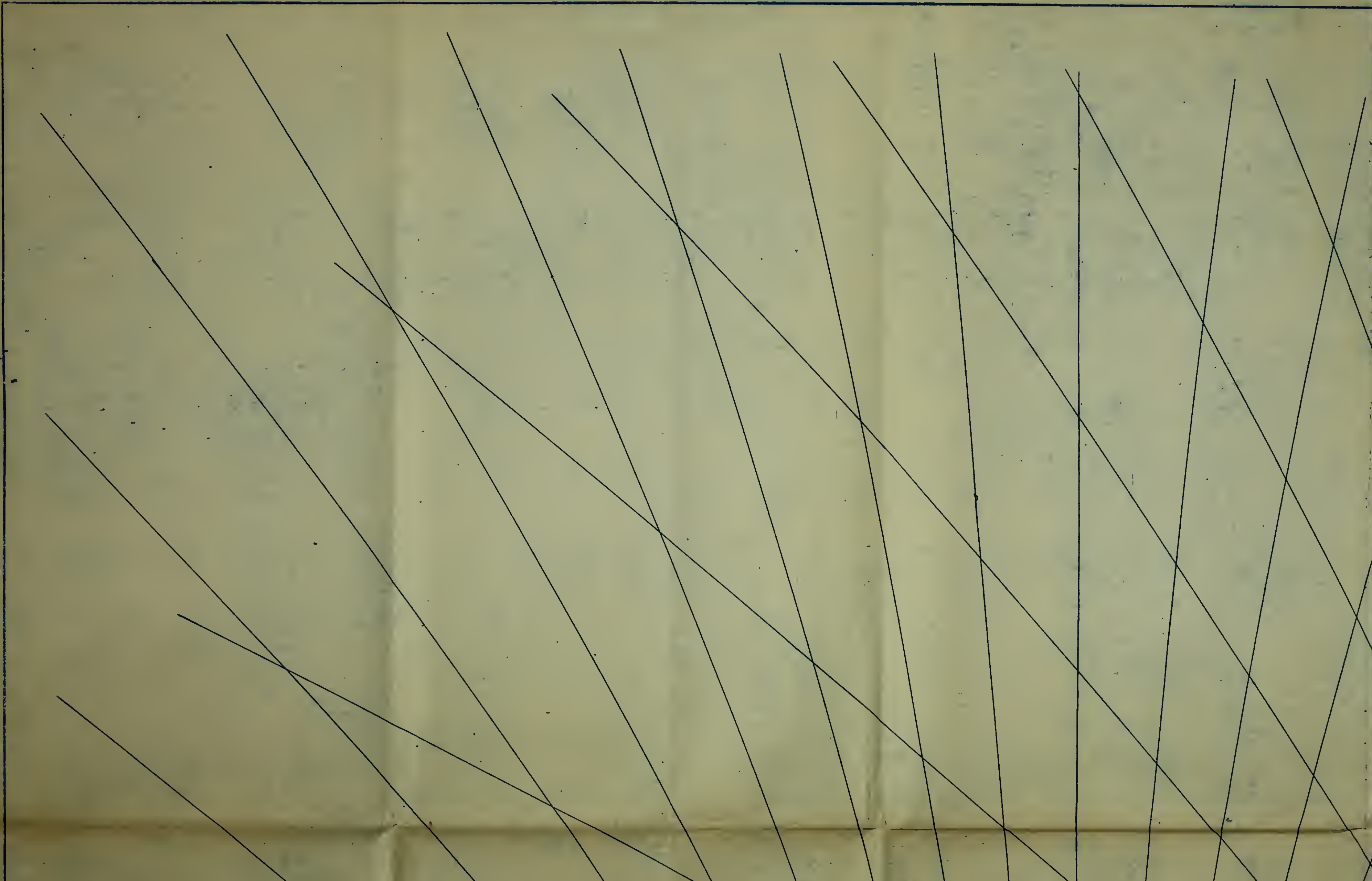
SK. No. 22

BE SURE THAT ALL OVERSIZE PLATES  
DIAGRAMS, CHARTS, ETC.) ARE FOLDED TO  
PERMIT A FREE MARGIN FOR BINDING AND SO  
THAT ALL FOLDED EDGES ARE AT LEAST ONE-  
HALF INCH FROM THE EDGE OF REGULAR THE-  
SIS SHEETS. (NOTE THAT THIS IS TRUE IN  
HARRISON'S THESIS IN THE FIRST FOLDED  
ILLUSTRATIONS BUT NOT IN ALL)

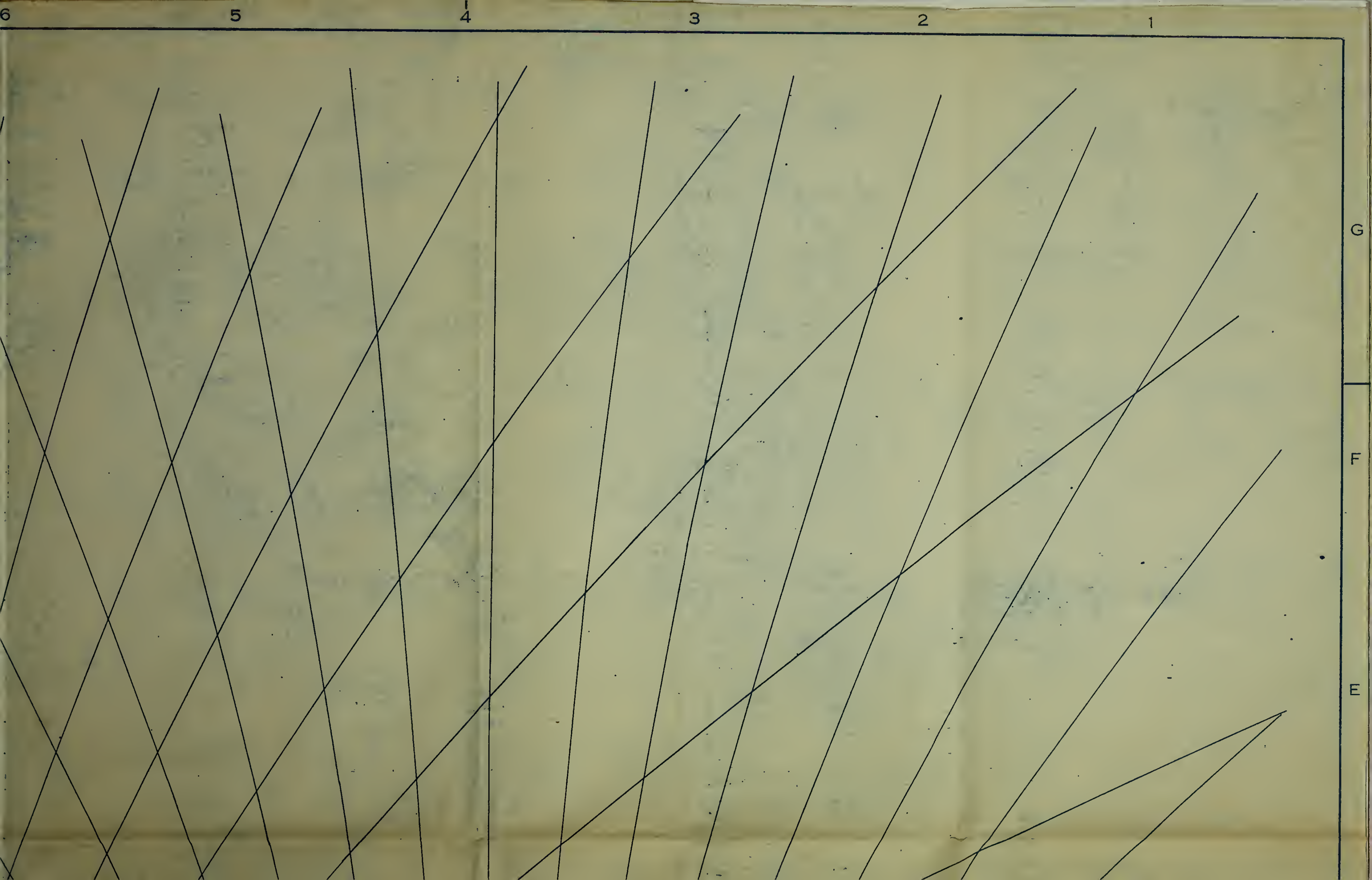
G

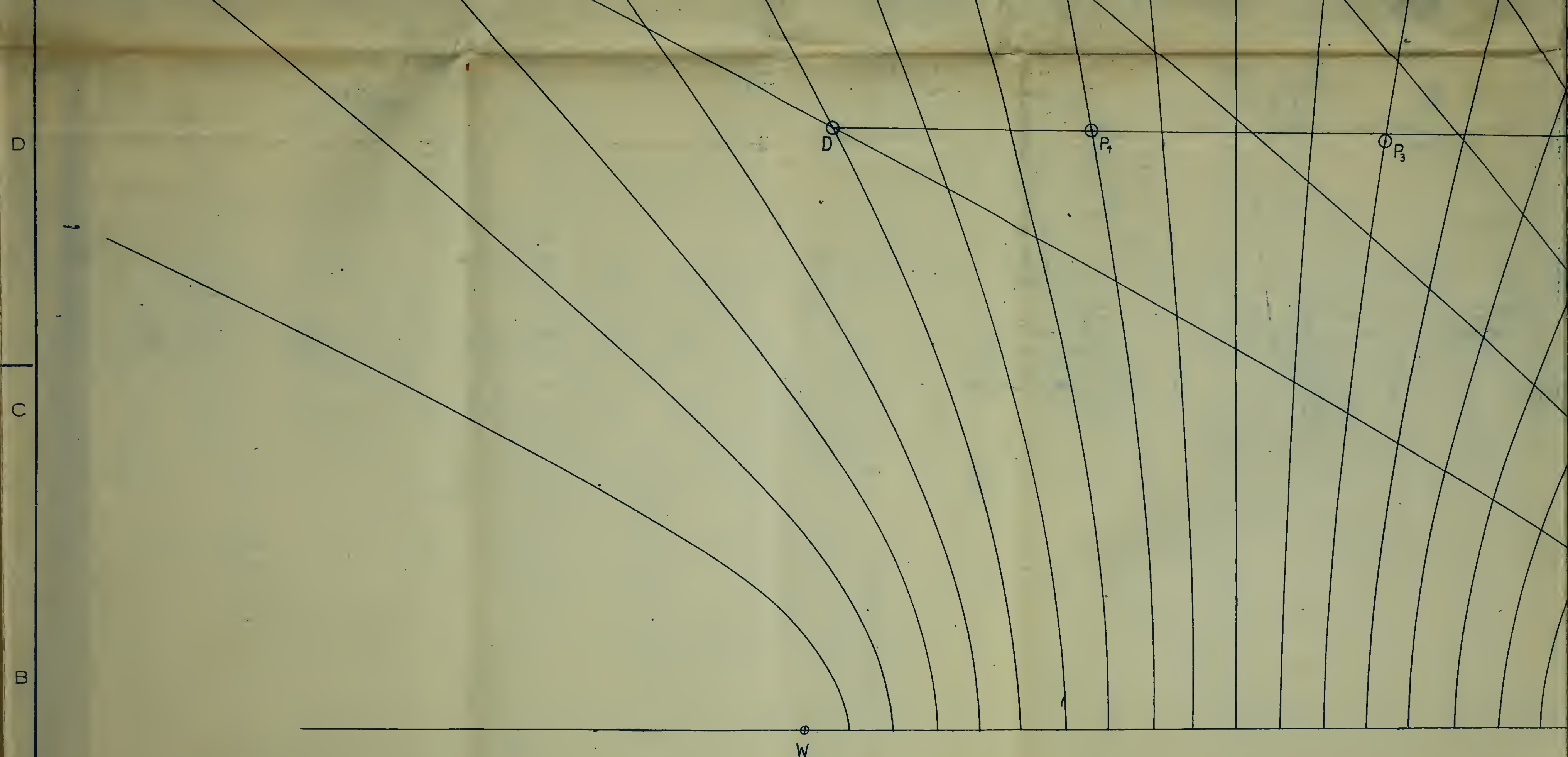
F

E





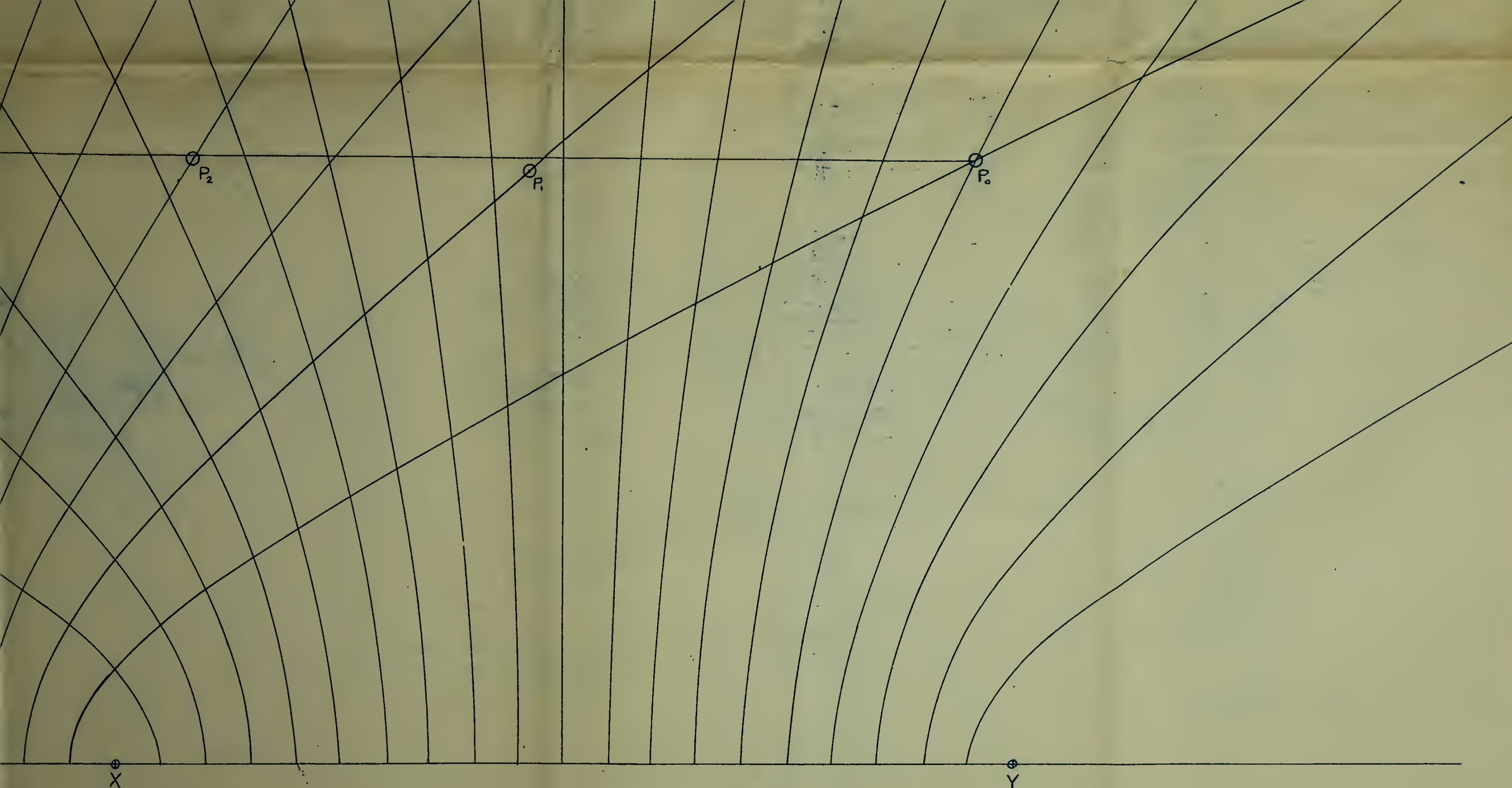




D  
C  
B  
A

TOLERANCES ON DIMENSIONS NOT OTHERWISE SPECIFIED			GROSS WT. LBS.....
DECI. DIM.	FRAC. DIM.	ANG. DIM.	SCALE.....



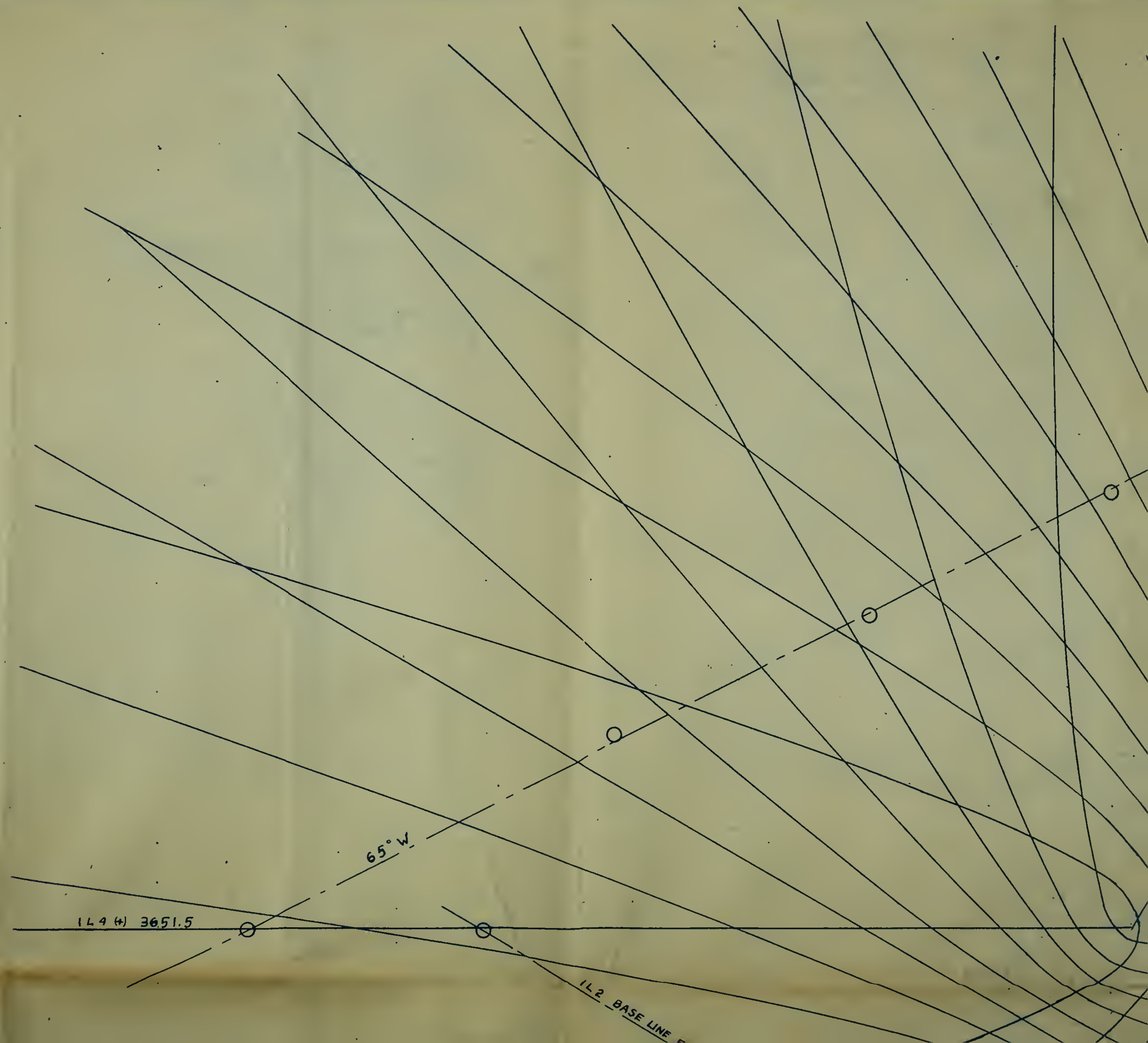


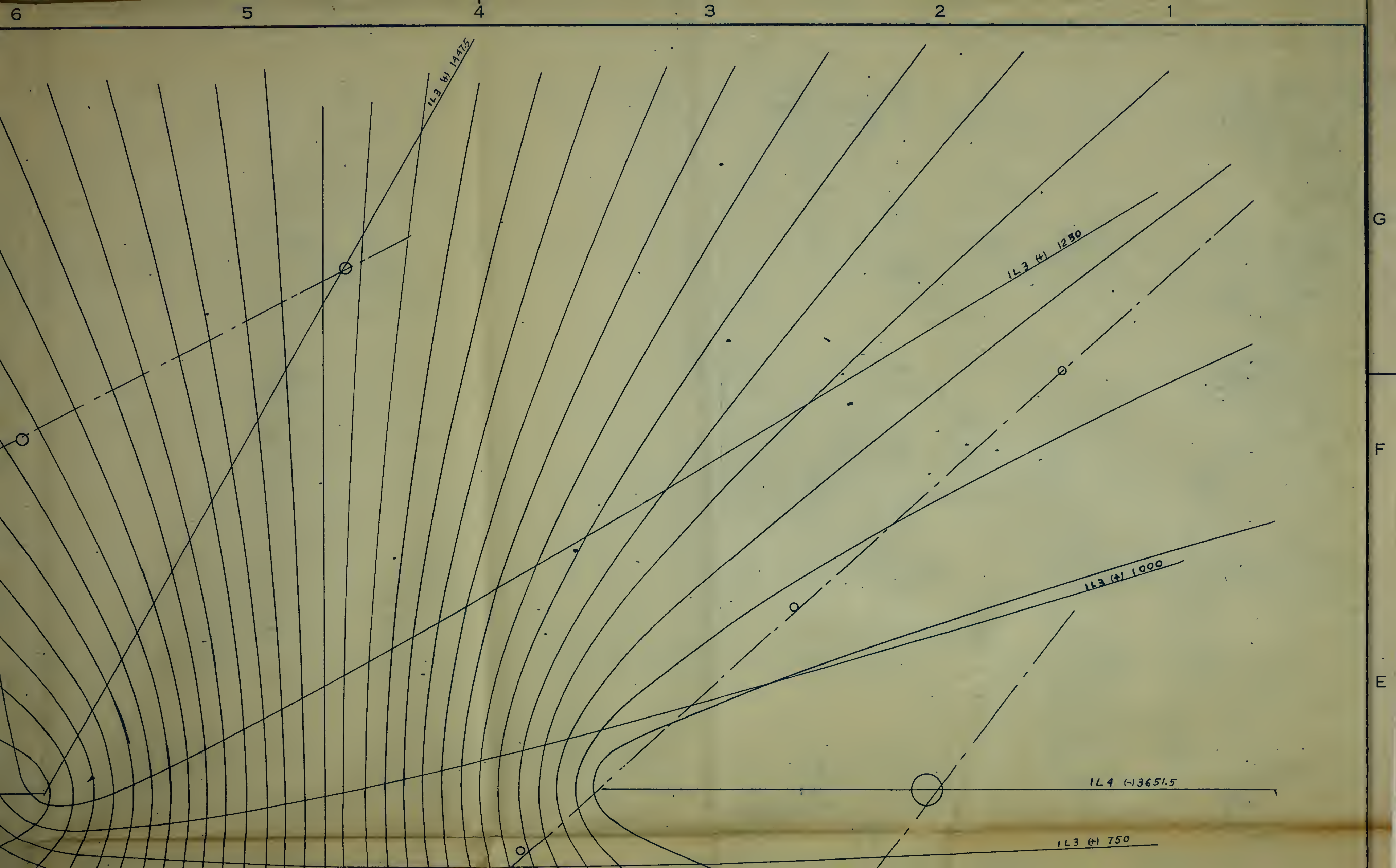
VECTOR COMPUTER TRACK IN PLANE	
FIG 23	
SPECIAL CONTRACT REQUIREMENTS	
REFERENCE DRAWING NUMBER	

DRAWING NUMBER	REV. SUB-LETTER
----------------	-----------------

A  
B  
C  
D

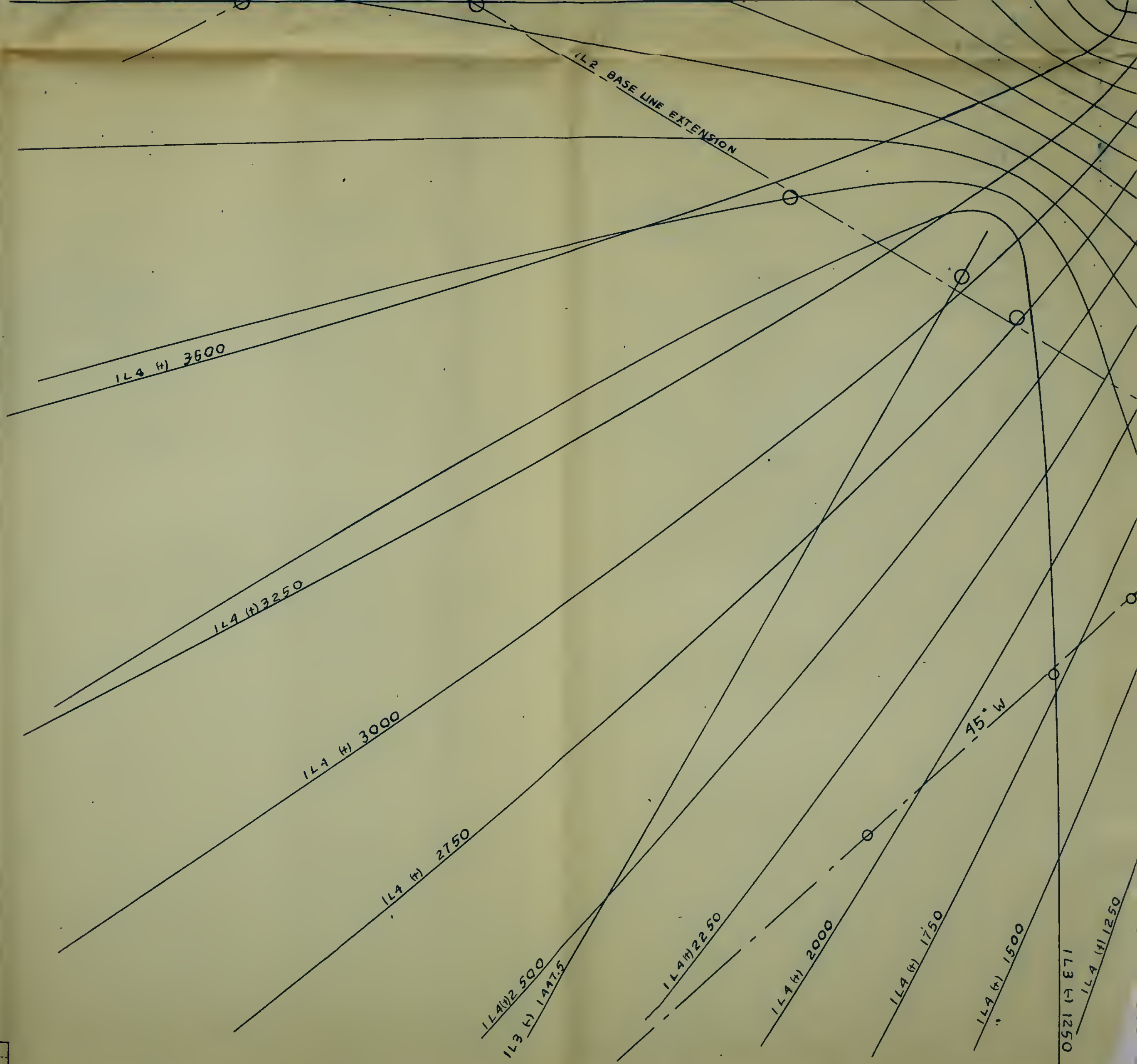




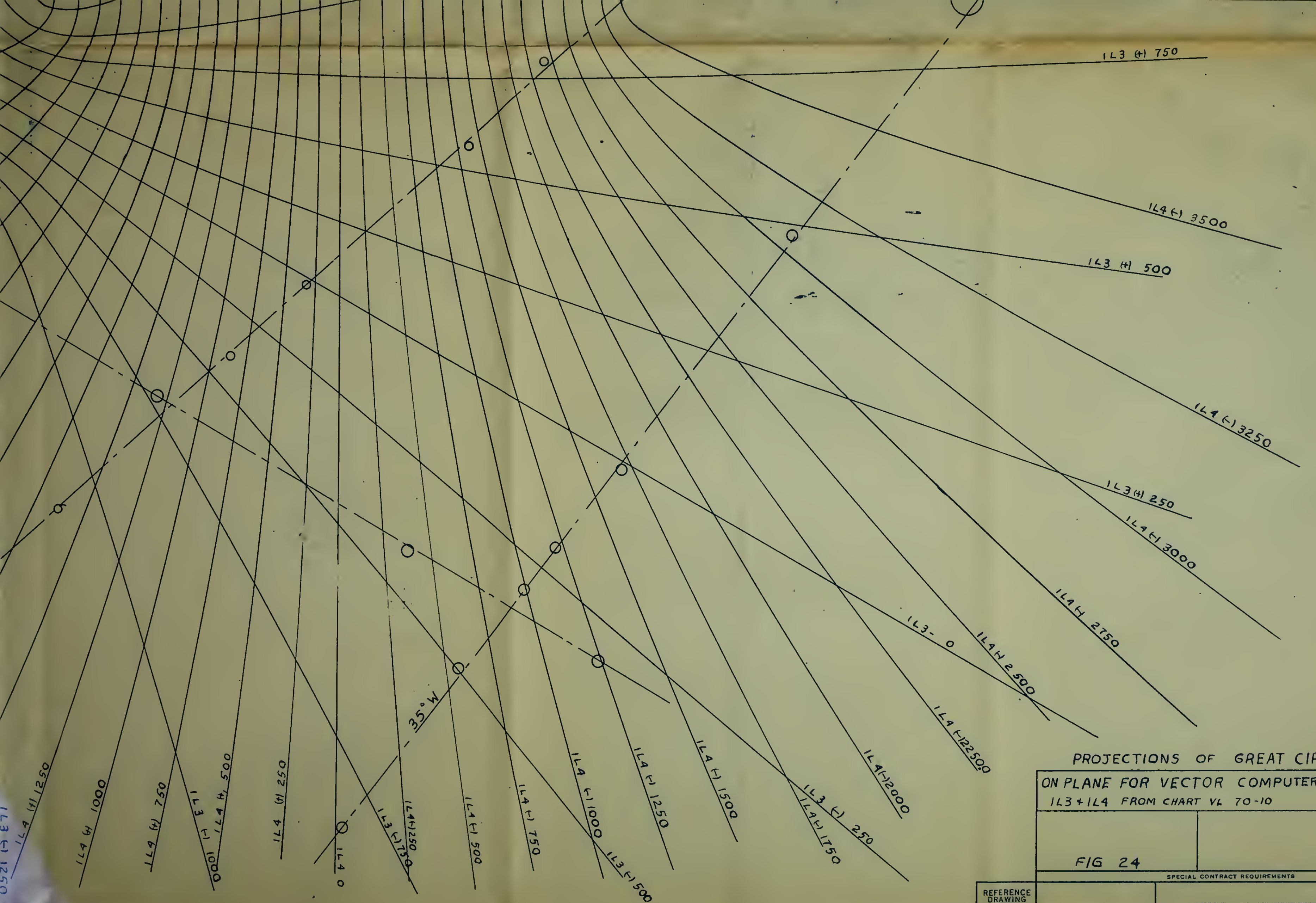




D  
C  
B  
A



TOLERANCES ON DIMENSIONS NOT OTHERWISE SPECIFIED			GROSS WT. LBS.
DECI DIM	FRAC DIM.	ANG. DIM.	



PROJECTIONS OF GREAT CIRCLES  
ON PLANE FOR VECTOR COMPUTER USING  
1L3 + 1L4 FROM CHART VL 70-10

FIG 24

REFERENCE  
DRAWING  
NUMBER

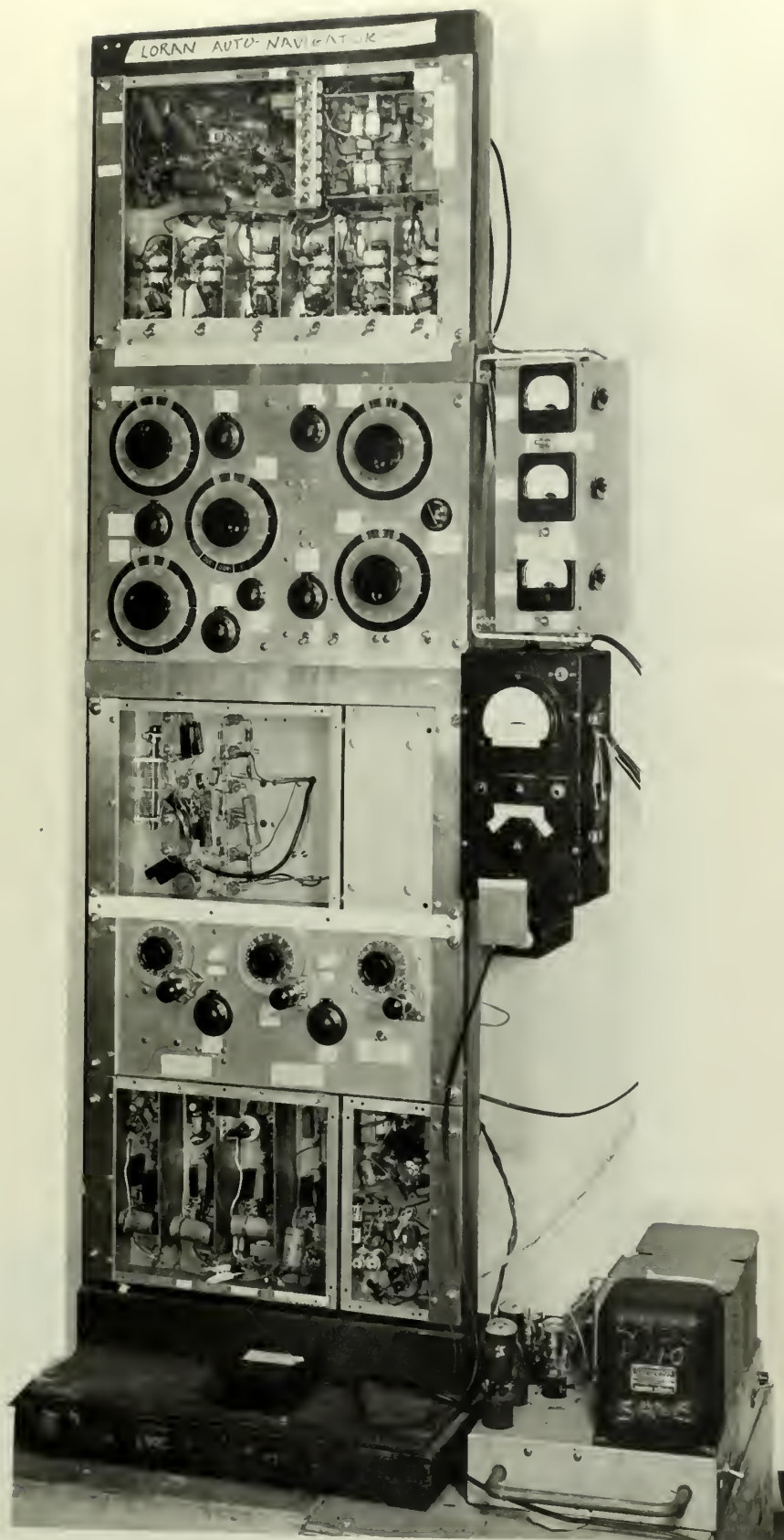
SPECIAL CONTRACT REQUIREMENTS

REV. SUB-LETTER	
DRAWING NUMBER	

D  
C  
B  
A





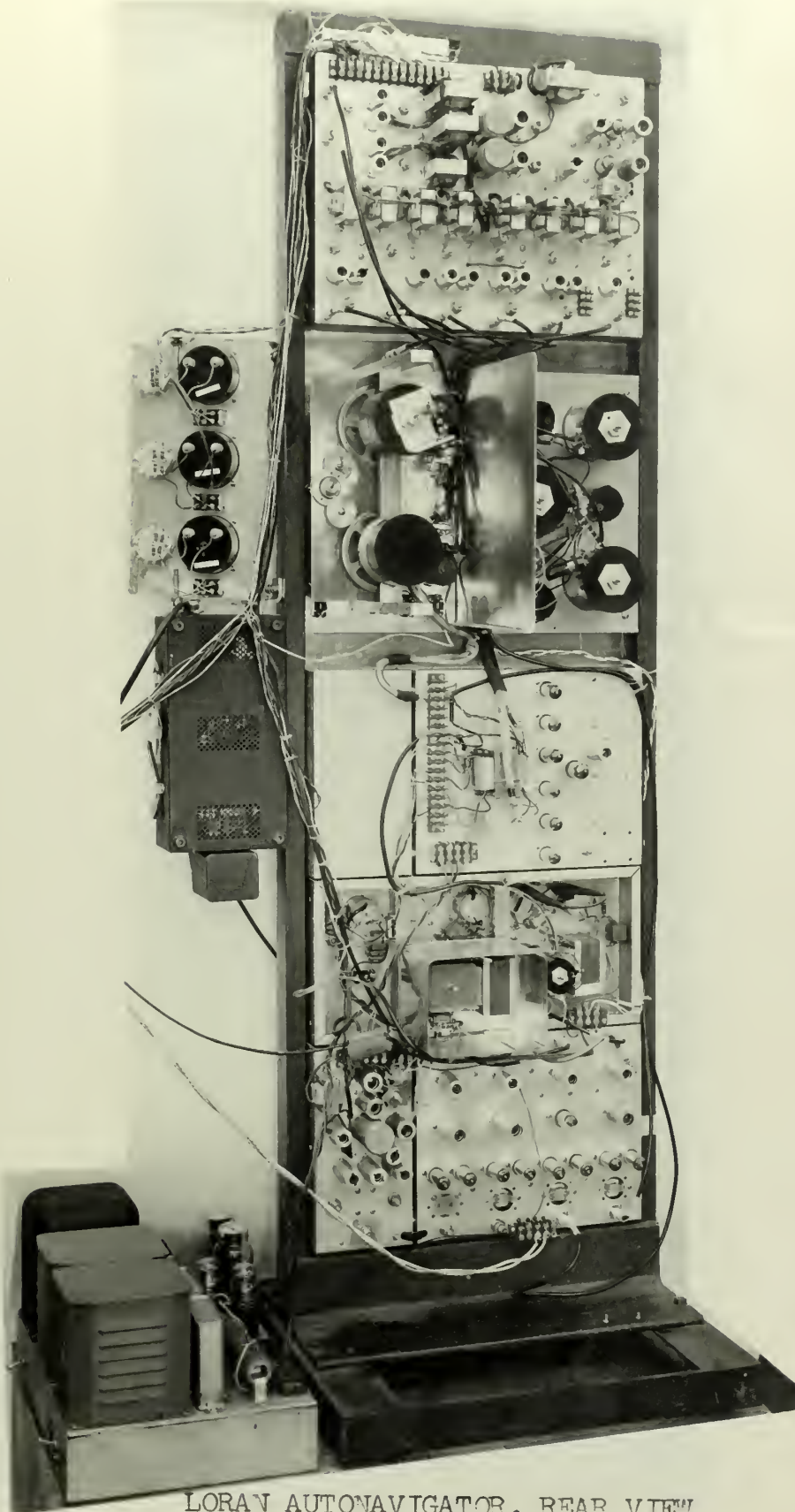


LORAN AUTONAVIGATOR, FRONT VIEW

FIGURE XXV

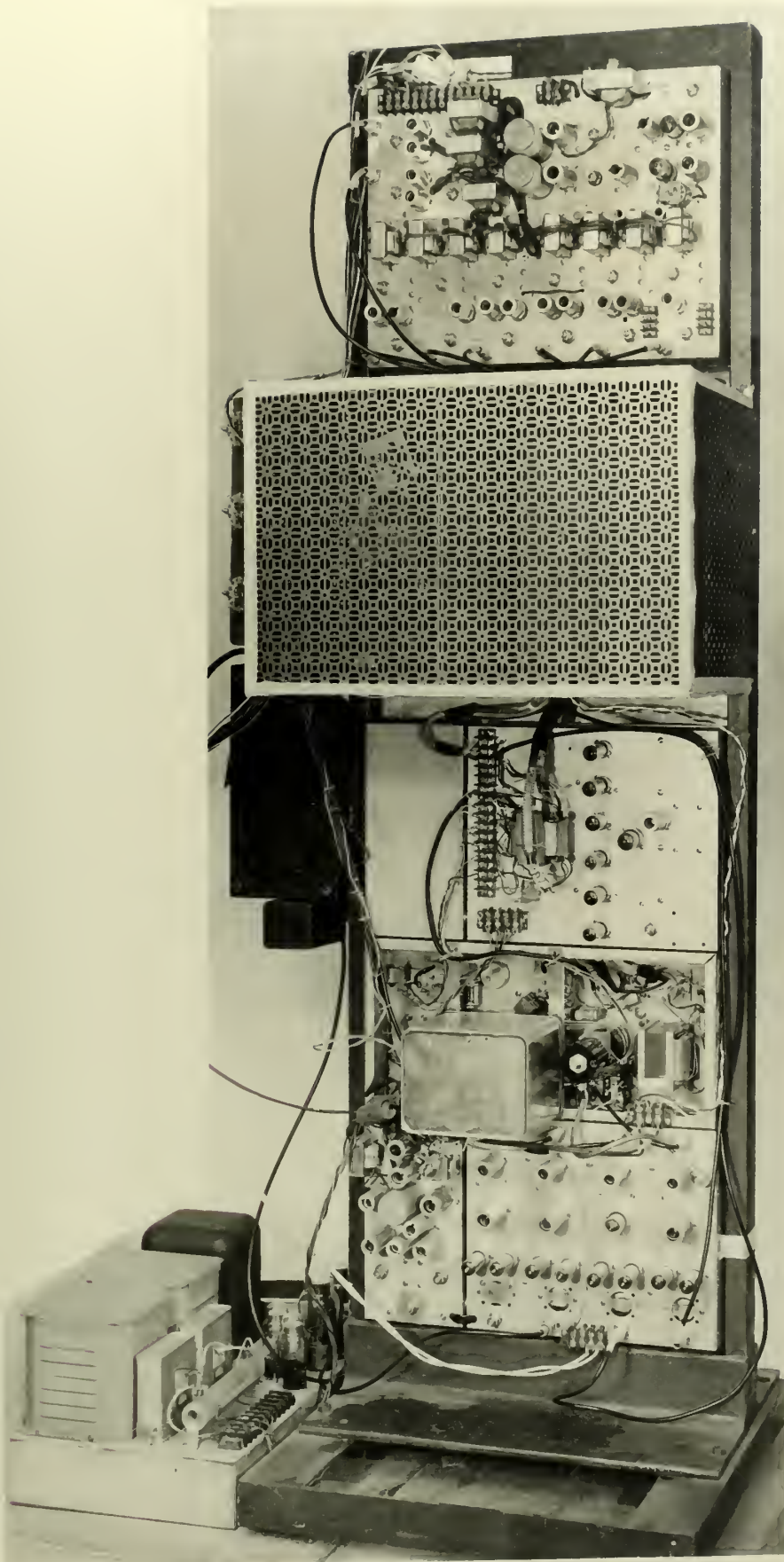






LORAN AUTONAVIGATOR, REAR VIEW  
SHIELDS REMOVED





LORAN AUTONAVIGATOR, REAR VIEW

FIGURE XXVII













DE 1159  
29 JUL 68  
16 NOV 70  
19 NOV 71

5283  
16833  
19452  
19974

Thesis  
T46

13109  
Thorsson, W. M.  
Hyperbolic auto-navi-  
gation.

DE 1159  
29 JUL 68

5283  
16833  
19452

thesT46

Hyperbolic auto-navigation.



3 2768 002 03523 0

DUDLEY KNOX LIBRARY